



DEPARTMENT OF BIO-MEDICAL ENGINEERING

---

NON-CONTACT STRAIN DETERMINATION OF CELL  
TRACTION EFFECTS

---

By

NIVEDITHA SATHIAMOORTHY (201180268)

THIS THESIS IS SUBMITTED IN PARTIAL FULFILMENT  
OF THE REQUIREMENTS FOR THE DEGREE OF MSc IN  
BIOENGINEERING

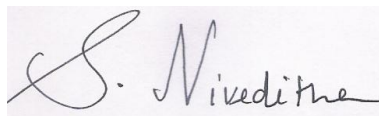
JANUARY-2013  
BIOENGINEERING UNIT  
UNIVERSITY OF STRATHCLYDE  
GLASGOW, UK

# DECLARATION OF AUTHENTICITY AND AUTHOR'S RIGHTS

This thesis is the result of the author's original research. It has been composed by the author and has not been previously submitted for examination which has led to the award of a degree.

The copyright of this thesis belongs to the author under the terms of the United Kingdom Copyright Acts as qualified by University of Strathclyde Regulation 3.50. Due acknowledgement must always be made of the use of any material contained in, or derived from, this thesis.

Sign:

A handwritten signature in black ink on a light-colored background. The signature is written in a cursive style and reads "S. Niveditha".

Date:

# ACKNOWLEDGEMENT

First and foremost, I would like to thank God, the Almighty for granting me the capability and strength to pursue the MSc course in Bio-engineering.

It gives me immense pleasure to express my gratefulness to my esteemed supervisor, Dr. Richard Black, senior lecturer, Department of Bio-engineering (Wolfson centre), University of Strathclyde, Scotland, for the patient guidance, valuable suggestions and friendly mentorship he provided me all the way through this MSc project.

I wholeheartedly thank my friends and family for their constant inspiration and support throughout this work.

My sincere thanks to the University of Strathclyde, Scotland for providing me the opportunity and support required all through my academic pursuit.

## ABSTRACT

Irreversible tissue damage leading to organ failure is a common health problem in today's world. Regenerating these damaged tissues with the help of scaffolds is the solution offered by tissue engineering. In cases where the extra-cellular matrix (ECM) is to be replaced by an artificial substrate (scaffold) or matrix, cellular traction forces (CTF) are exerted by the cells on the scaffold surface. An ideal scaffold should exhibit mechanical characteristics similar to those of the ECM it is intended to replace. In other words, the capacity of a scaffold to withstand deformation should be comparable to that of a natural ECM. And with knowledge of those forces and deformations the properties of the scaffolds may be inferred. Digital Image Correlation (DIC), a non-contact image analysis technique enables us to measure point to point deformation of the scaffold by comparing a sequence of images captured during the process of scaffold deformation. This review discusses the methodology involved and implementation of DIC to measure displacements and strain.

*KEYWORDS*

Cellular Traction Forces

Scaffolds

Digital Image Correlation

Non-contact strain

Interpolation

Image correspondence

Sub-pixel comparison

*ABBREVIATIONS*

CTF – Cellular traction forces

ECM – Extra cellular Matrix

DIC – Digital image correlation

3D – Three dimensional

2D – Two dimensional

# TABLE OF CONTENTS

DECLARATION OF AUTHENTICITY AND AUTHOR'S RIGHTS .....	i
ACKNOWLEDGEMENT .....	ii
ABSTRACT .....	iii
KEYWORDS AND ABBREVIATIONS .....	iv
TABLE OF CONTENTS .....	v
LIST OF FIGURES.....	viii
LIST OF TABLES .....	x
1. INTRODUCTION.....	1
1.1 Overview of the thesis .....	3
2. BACKGROUND.....	5
2.1 Significance of cellular traction forces .....	5
2.2 Significance of mechanotransduction.....	7
2.3 Significance of scaffolds .....	9
2.4 Significance of strain measurement on scaffolds .....	13
2.5 Non-contact methods for strain analysis.....	14
2.6 DIC for non-contact strain analysis .....	14
3. METHODOLOGY.....	18
3.1 Digital image correlation.....	18
3.1.1 2D DIC .....	18
3.1.2 3D DIC .....	21
3.1.3 Comparison between 2D DIC and 3D DIC .....	24
3.1.4 Assumptions in DIC .....	25

3.1.5 Procedure of DIC.....	26
3.1.5.1 Preparation of specimen for DIC .....	26
3.1.5.2 Image acquisition.....	29
3.1.5.3 Image pre-processing.....	35
3.1.5.4 Image processing .....	37
3.1.5.5 Image post processing .....	46
4. IMPLEMENTATION OF DIC .....	52
4.1 Macroscale implementation.....	52
4.1.1 On biological specimens (on bones).....	52
4.2 Microscale implementation .....	54
4.2.1 On biological tissues.....	54
4.2.2 On artificial substrates .....	57
4.3 On other specimens .....	58
5. PROBLEMS ENCOUNTERED IN DIC .....	60
5.1 Fundamental problems in DIC .....	60
5.1.1 Aperture problem.....	60
5.1.2 Correspondence problem.....	61
5.2 Practical problems in DIC .....	62
5.2.1 Improvement in accuracy .....	62
5.2.2 Out of plane displacements.....	63
5.2.3 Lens aberration .....	63
5.2.4 Computational efficiency .....	64
5.3 Errors in DIC .....	65

5.3.1 Errors due to speckle pattern .....	65
5.3.2 Errors due to intensity interpolation .....	65
5.3.3 Errors due to experimental setup and DIC algorithms.....	66
6. CONCLUSION .....	68
7. FUTURE WORK .....	69
7.1 Optimised specimen surface preparation.....	69
7.2 Improvement in image acquisition .....	69
7.3 Optimisation of image registration .....	69
7.4 Image processing .....	70
7.5 Algorithms and schemes.....	70
7.7 Improvement in strain and displacement measurement accuracy.....	71
REFERENCES.....	72



## LIST OF FIGURES

Figure 1-1 Tissue engineering approach [1].....	2
Figure 1-2 Overview of the thesis.....	4
Figure 2-1 Schematic representation of a migrating cell and the tractions it generates on the substrate [2].....	6
Figure 2-2 Cellular processes of mechanosensing and responses (Vogel et al., 2006).....	8
Figure 2-3 Different approaches of scaffold fabrication [3].....	11
Figure 2-4 Bone cells attached to scaffolds by extending cell processes to the surface [4].....	12
Figure 2-5 Osteoblast cells seeded on nano-fiber scaffolds [5].....	12
Figure 2-6 Cells seeded on a 3D scaffold [6].	13
Figure 2-7 Speckle interferometry (Saleem et al., 2005).	15
Figure 2-8 Laser extensometers [7] and [8]	16
Figure 3-1 Representation of consecutive images of a deforming subset with respect to time (Cofaru et al., 2012)	18
Figure 3-2 Grayscale correlation of undeformed and deformed sub-image.	19
Figure 3-3 Experimental setup for 2D DIC.	21
Figure 3-4 Experimental setup for 3D DIC [20].	23
Figure 3-5 2D and 3D image acquisition using cameras as input devices (Heinz et al., 2010).....	25
Figure 3-6 Overall concept of DIC [21].....	26
Figure 3-7 Randomly distributed fluorescent particles inside a reference subset are automatically identified and marked as a series of rectangular windows (Huang et al., 2010)	28
Figure 3-8 A typical speckle pattern [9].....	29
Figure 3-9 Speckle pattern on aortic specimen used for DIC analysis [10].	29

Figure 3-10 CCD and CMOS cameras [11] .....	31
Figure 3-11 Stereomicroscope coupled with digital camera system [12].....	32
Figure 3-12 Micro CT scanner [13] and [14] .....	33
Figure 3-13 Electron microscope [15] and [16]. .....	34
Figure 3-14 Confocal microscope [17] and [18]. .....	35
Figure 3-15 Interpolation schemes [19] .....	45
Figure 3-16 Grayscale interpolation.....	45
Figure 3-17 RGB interpolation- comparison of non-adaptive interpolation methods (Prajapati et al., 2012).....	45
Figure 3-18 Concept of displacement measurement in DIC(Tang et al., 2012).....	47
Figure 3-19 Strain measurement concept in DIC (Tang et al., 2010).....	49
Figure 3-20 3D displacement and strain map.....	50
Figure 3-21 Process of scaffold evaluation using digital image correlation.....	51
Figure 5-1 Aperture problem (Sutton et al., 2009).....	61
Figure 5-2 Correspondence problem (Sutton et al., 2009). .....	62

## LIST OF TABLES

Table 1 Commonly used correlation criteria (Pan et al., 2009).....	40
Table 2 Correlation criteria used in DIC to evaluate the similarity degree between reference and target subset (Pan, 2011).....	41

# 1 INTRODUCTION

Cellular traction forces are fundamental to many cellular physiological processes: both developmental and pathological. For example, in order to enable migration, a cell interacts with the physical environment surrounding it through the application of these cell traction forces (CTF) (Wang et al., 2010). The consequence of this action is the deformation of the cell and the substrate lying under it. These mechanical forces causing deformations could be in the form of stretch, pressure, flow, shear, loads, etc., and are generated through interactions between actin and myosin within the cell cytoskeleton. These forces are translated into bio-chemical signals in a process known as mechano-transduction, resulting in many cellular functions such as DNA synthesis, cell differentiation, and proliferation (Ingber, 2006).

Tissue damage following death or injury of the fundamental unit of the body “cell” leading to organ failure is a common health problem. All tissues in the body have the property of regeneration but the failure of regeneration due to some pathology leads to scar formation. Wound healing is an intricate process involving various phases. The immediate response of an injury being coagulation, followed by inflammation and wound contraction. Wound contraction is facilitated by accumulation and contraction of the fibroblasts on collagen fibrils, resulting in shearing forces on the ECM leading to wound contraction (Gabbiani et al., 1971; Majno et al., 1971). Each cell in the body has complex forms of intercellular communication and chemotactic activity for establishing the process of regeneration which leads to healing. When this form of communication through the ECM is altered, for example, in cases like diabetes or autoimmune diseases, the healing process is delayed (Yoshihiro Abiko and Denis Selimovic). Extra-cellular matrix (ECM), the outer membrane, which interacts constantly with the outside environment, is the first component to get damaged or altered during such injury. The damage of ECM prevents the cell to perform basic functions, which ultimately leads to symptoms of disease. Tissue engineering is a diverse field that combines the principles of both engineering and life sciences to produce tissue substitutes that facilitate tissue regeneration. This field

addresses this problem by developing artificial substrates (scaffolds) that replace or augment the natural ECM.

.....  
**Figure 1-1** Tissue engineering approach 1.Donor cells from tissue 2.Tissue culture 3.Cells seeded on scaffolds 4.In-vitro tissue culture on scaffold 5.In-vivo implantation of cell seeded scaffold [1]. [biomed.brown.edu](http://biomed.brown.edu)

Scaffolds are porous artificial structures that replace the natural ECM and serve as a basic framework for tissue regeneration. A scaffold should satisfy four design criteria to match the characteristics of a natural ECM, namely: the scaffolds should be bio-compatible and bio-degradable; they should have high porosity; they should promote cell adhesion, growth, proliferation and differentiation; and they should have mechanical properties similar to the natural substrate (ECM). The fourth property is arguably the most relevant to the subject of this thesis, since it provides the means by which we can infer the forces that a cell exerts on its surrounding matrix. For instance the traction forces exerted by tissue cells when cultured on very thin sheets of a silicone membrane have been observed in the form of elastic distortion or wrinkles on the substratum (Harris et al., 1980). The magnitude of the forces exerted by individual cells on a Poly-dimethylsiloxane (PDMS) substratum has been quantified using a photoelastic method (Curtis et al., 2007).

Strain (the amount to which a scaffold deforms) is a physical entity which depends on the elastic properties of a scaffold, i.e., it explains the capacity of a scaffold to withstand deformation in response to externally applied forces. Thus, by measuring strains (deformations) that are evident on a scaffold, we may infer the mechanical properties of that scaffold. There are various methods of measuring contact strains, but such methods cannot be used to measure micro strains over a microscopic textured surface. This is because it requires direct contact with the scaffold during measurement, which may lead to inaccurate results if proper fixation of the scaffold is not achieved. Also this method requires time-consuming surface preparation. In order to overcome the deficiencies of these methods it would be desirable to develop a non-contact method for measuring the strains evident on the scaffolds. One approach is the use of the image analysis technique, Digital Image Correlation (DIC), which offers a relatively high precision strain measurement and consumes very little processing time. Hence this review focuses on the use of DIC technique to measure microscopic strains on these scaffolds. Also strain measurements (from macroscopic to microscopic scale) in diverse specimens were reviewed.

## 1.1 Overview of thesis

Chapter 2 provides the background information about the significance of cellular traction forces, mechano-transduction and the scaffolds, explains the need for measuring strain on scaffolds and discusses various other methods and the widely used Digital Image Correlation (DIC) technique utilised for non-contact strain analysis. Chapter 3 demonstrates the methodology for measuring displacements and strains using digital image correlation method.

Chapter 4 illustrates the implementation of digital image correlation method on various types of specimens ranging from macroscale to microscale. Chapter 5 elucidates the problems encountered in digital image correlation technique. Finally, Chapter 6 concludes with suggestions for possible extensions of this research.

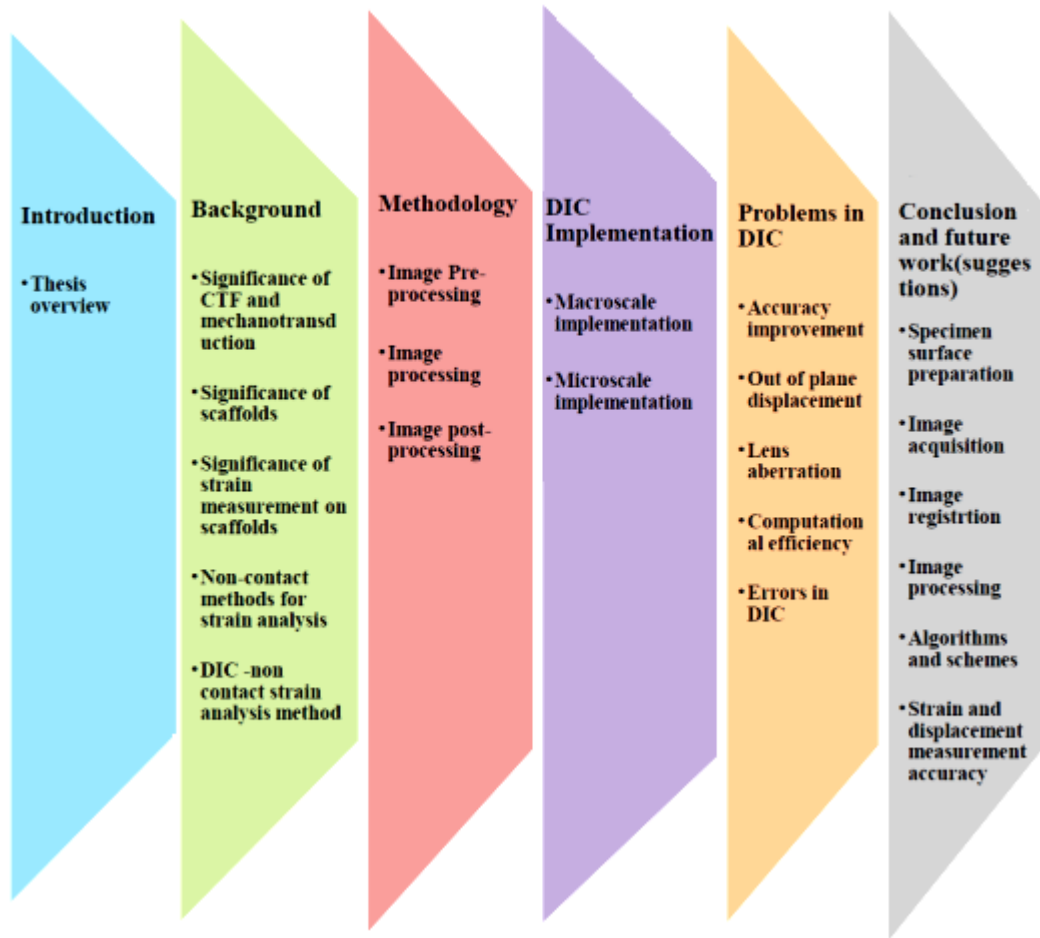


Figure 1-2 Overview of the thesis

## 2 BACKGROUND

A basic overview of the significance of cellular traction forces, mechanotransduction, scaffolds and image processing techniques are explained for a better understanding of the comparisons and discussions made in this review.

### 2.1 Significance of cellular traction forces

The cellular traction force is the force exerted by the cell on the extracellular matrix, when it translocates the bulk of the cell (Ananthakrishnan et al., 2007). Thus it is clear from this statement that the each cell in our body develops a force in order to move forward. It is this cell movement (cell migration) induced by the cellular traction forces, is the basic behaviour of the cell that governs many of the important cellular functions within all living organisms. Maintenance of cellular homeostasis, cell shape control, cell differentiation, DNA synthesis, ECM protein secretion, morphogenesis, embryogenesis, angiogenesis, wound healing, cancer metastasis represent a few of the many cellular mechanisms that depend on CTF (Wang et al., 2010).

These cellular traction forces leading to cell migration occurs within every living organism throughout its life span, i.e., from the formation of embryo till death. For example: cell migration in early embryo stage helps in the formation of germ layers during embryogenesis; cell migration (movement of dividing cells in layers) to specific regions helps in formation of tissues and organs in adults during morphogenesis; migration of vascular endothelial cells helps in the formation of new capillaries during angiogenesis; migration of macrophages, neutrophils and fibroblast cells into wound sites helps in wound healing; leukocyte migration into inflammation sites plays an important role in creating an inflammatory response; uncontrolled leukocyte migration leading to diseases such as asthma and rheumatoid arthritis; and the migration of primary tumour cells to other healthy sites of body leading to infection (tumour metastasis).



Cellular traction forces constantly re-model and re-structure the cell and the ECM (tissue patterning) and are essential to homeostasis. Thus, both developmental processes (formation of tissues and organs) and disease states (tissue injuries and organ malformation and malfunction) occurring in our body may be viewed as a consequence of these cellular traction forces, an argument which is explained by Mammoto et al., (2010).

In general, a cell is mechanically attached to both the substrate (ECM) lying under it and its neighbouring cells which leads to an interaction between them (cell to cell and cell to ECM). Thus both cell-substrate interactive forces and cell-cell interactive forces contribute for the generation of the total traction force. The relationship between these forces is explained by Maruthamuthu et al., (2011) who argued that these forces are regulated by the bio-chemical and bio-mechanical properties of the cell substrate. In other words, the properties of the ECM indirectly influence the cell behaviour. This is a coupled process whereby changes to the ECM in response to cellular traction forces, in turn, alter the cell functions. Thus the cellular traction forces exerted on the substrate (ECM) naturally become a physical determinant of tissue formation, re-modelling, functioning, injury and death.

.....

**Figure 2-1** Schematic representation of a migrating cell and the tractions it generates on the substrate. [2]

[cellmigration.org](http://cellmigration.org)

## 2.2 Significance of mechano-transduction

All cells in living organisms experience cellular traction forces in one way or another, as discussed above. Apart from these forces, cells are also subjected to different types of mechanical loads (both external and internal loads) microscopically in the form of pressure, flow, stress, strain, etc., during normal physical activities, for example, during digestion, muscular contraction, hearing, touch, injury, and balancing. These mechanical signals are sensed (mechano-sensing) and converted into bio-chemical signals by cells. These processes play an important role in organ development and maintenance of homeostasis by controlling the cell growth and functions. The role of mechano-transduction in the context of bone repair and regeneration (physical adaptation of bone and fracture healing), has been reviewed by Huang and Ogawa (2010). The influence of intra- and extra-cellular forces on the structure of nucleus, and cellular signalling and function, in particular, has been discussed by Dahl et al., (2008). McCain et al. (2011) describes the effects of mechano-transduction in cardiac cellular environment (i.e., within myocytes inside heart) whereas the article by Hahn and co-worker (2009) addresses the significance of mechano-transduction in vascular physiology (blood flow mechanisms), which is essential for detection of blood vessel growth, functioning and dysfunction.

In short, mechano-transduction is a cascade of multiple processes involving mechano-sensing, mechano-transduction and mechano-response that explains the influence of physical environment on biological environment. This cascade involves the sensation of mechanical signals with the help of mechanically gated ion channels (mechano-sensing) followed by the excitation of the sensory neurons and stimulation of the mechano-receptors which induces the ion-channels of the cell membrane (ECM) to open, which is further followed by the production of transduction current resulting in the change in membrane potential of the cell (mechano-transduction). This change in membrane potential alters the morphology of the cell (mechano-response) ultimately changing the cell behaviour and functions. Ingber (2006) gives a clear account of this cascade (mechano-chemical conversion) as it occurs in the auditory system.

A number of components are involved during the entire process of mechano-transduction. It includes transduction elements such as ECM, cell-cell adhesions and cell-ECM adhesions, membrane components, cytoskeleton filaments, nuclear components and surface processes (Ingber et al., 2006). Any alteration in this cascade (changes attributed to cell mechanics, structure of ECM and cytoskeleton and molecular mechanisms concerned to mechano-sensing) leads to abnormal mechano-transduction. A list of diseases (e.g., atherosclerosis, asthma, osteoporosis, heart failure, cancer etc.) that may be attributed to abnormal mechano-transduction, and a list of corresponding therapies (achieved by alteration of mechano-transduction) that have been applied in an attempt to cure these diseases, is described in the article by Ingber (2003).

.....  
**Figure 2-2** Cellular processes of mechanosensing and responses (Vogel et al., 2006)

### 2.3 Significance of scaffolds

As discussed in the preceding section, the ultimate cause for any disease or tissue injury or trauma occurring in living organisms is mediated, in part, to the failure of mechano-transduction processes at a cellular level. Thus the regulation of this processes is highly required to promote the development of an organism at each and every level, i.e., dysfunction of cells (cellular level) leads to degeneration of tissues

(tissue level), which, in turn, leads to organ failure (organ level), resulting, eventually, in death of the organism (organism level).

Failure of this process is often characterised at the cellular level by alterations in the cell along with its underlying substrate (ECM). Of the two, the latter is more likely to have the greatest impact since the ECM is the physical determinant of tissue development, which anchors the living cells and facilitates the inter-cellular communication of mechanical information without which mechano-transduction is impossible (Ghosh et al., 2007).

This necessitates the regeneration of ECM, which is the only way to promote cell growth and matrix production to replace the lost ECM with a newly re-generated ECM. In order to complement this naturally-occurring process, scaffolds (artificial ECM) may be introduced. Scaffolds are the three-dimensional, porous and membranous structures made of natural or synthetic materials (mostly polymers) that mimic the characteristics of a natural ECM and acts as a template (a basic framework) in order to promote tissue growth and development. These structures assist the growth of cells, whether seeded on the scaffold prior to implantation, and/or growing into the scaffold thereafter, by providing temporary support while the new matrix is laid down and the scaffold degrades (Ghosh et al., 2002)

An ideal scaffold should possess the characteristics of a natural ECM exactly. The analogous functions of ECM in native tissues and scaffolds in engineered tissues have been compared by Chan et al., (2008), who explain the difficulty in generating an ideal scaffold in terms of the inability of the a given biomaterial to reproduce the complex composition and dynamic nature of natural ECM in practice. Even though an ideal scaffold may not exist, there are some basic requirements that must be met, such as bio-compatibility, bio-degradability, mechanical properties, architectural organisation, and ease of manufacturing (O'Brien et al., 2011), which must be satisfied if the chosen scaffold is to adapt to the biological environment to which it is exposed.

Polymers are widely considered to satisfy many of the demands of tissue engineering because of their physical and mechanical properties, processability and

biocompatibility. Some of the more commonly-used synthetic are bio-degradable polyesters (PGA, PLA, PLGA), polyanhydride, polyorthoester, polycaprolactone, polycarbonate and polyfumarate; and polymers of biological origin, i.e., the proteins of ECM (e.g., collagen, glycosaminoglycan, alginic acid, chitosan, polypeptides etc.), as documented by Chen (2002) and Dhandayuthapani et al. (2007). The most common techniques include: solvent casting, particulate leaching, gas foaming, phase separation, electrospinning, porogen leaching, fibre mesh, fibre bonding, self assembly, melt moulding, membrane lamination, freeze drying, and rapid prototyping (e.g., three-dimensional printing). For a more detailed description of these fabrication techniques, the reader is referred to the articles by Subia et al. (2010) and Dhandayuthapani et al. (2007).

Three-dimensional hybrid scaffolds that combine the properties of synthetic polymers with naturally derived polymers and hydroxyapatite (mechanical strength offered by synthetic polymers and hydrophilic property offered by naturally derived polymers and osteoconductivity offered by hydroxyapatite) are described by Chen et al. (2002). These scaffolds were found to possess better tissue formation characteristics (smooth cell seeding, better cell interactions and signal recognition, cell invasion and growth) than other types.

.....

**Figure 2-3** Different approaches of scaffold fabrication [3]

[nist.gov](http://nist.gov)

The architecture and chemistry of the scaffolds used in the design of tissue engineering scaffolds differs according to the type of tissue for which a repair or a replacement is required. A number of scaffold based tissue engineered blood vessels were used to address the problems related with cardio-vascular diseases (Grace et al., 2012). Liver tissue engineering utilised polymeric scaffolds in order to encounter the problem of severe hepatic failure (Kazemnejad et al, 2009). Tendon and ligament tissue engineering used hybrid scaffolds in order to facilitate better cellular attachment and proliferation with improved mechanical properties (obtained by coating the bio-degradable knitted polyester scaffolds with nano-fibres and collagen) applied to tendon and ligament tissue engineering (Sahoo et al., 2007)

.....

**Figure 2-4** Bone cells attached to scaffolds by extending cell processes to the surface. [4]

[itg.beckman.illinois.edu](http://itg.beckman.illinois.edu)

.....

**Figure 2-5** Osteoblast cells seeded on nano-fibre scaffolds [5]

[materialsviews.com](http://materialsviews.com)

.....

**Figure 2-6** Cells seeded on 3D scaffold [6]

[ozbiosciences.com](http://ozbiosciences.com)

## 2.4 Significance of strain measurement on scaffolds

Attachment of a cell with its underlying substrate (ECM) is the first phase of a cell's struggle for survival (cell development). It is only after the success of this phase that a cell is able to undergo all other phases of its development. Thus every developmental phase of a cell is guided by the natural ECM by way of providing a structural support and regulation of inter-cellular communication. This ensures that ECM forms to be the primary support for cell development. In cases where the ECM has been replaced as a result of trauma or disease, the amount by which a scaffold deforms is the most relevant mechanical property that must be considered.

From the instant cells are seeded onto the scaffold surface, the manner in which each cell interacts with its new environment, by means of cellular attachment, contraction, functioning and growth, is mediated by the properties of the scaffold. Moreover, the properties of the cell membrane, like selective permeability, receptor binding etc., are greatly dependant on the traction forces exerted by the cell. Therefore, the mechanical property of the scaffold should ideally mimic that of extracellular matrix, so that the cell membrane retains its properties after cell contraction, similar to its properties in a natural environment. Hence, calculating strain measurements on scaffolds is considered essential to determine or predict the suitability of a scaffold to support cell growth and proliferation.

## 2.5 Non-contact methods for strain analysis

In the past, several contact methods have been used to analyse strain. Recently, owing to the requirements of non-destructive strain testing, several new methods have been introduced. The most commonly used non-contact methods are discussed below.



Digital image correlation based strain analysis:

One among the most widely used form of measurement of micro displacements and strain mapping using Cell Traction Force Microscopes. This system works with the help of Image acquisition tools and Image processing. In most of the biological applications like scaffold strain analysis, where microscopic strain maps are required, this technique is the most suitable. This technique is discussed in detail below.

Speckle interferometry:

Speckle interferometry works on basis of LASER beam interference that arises at surfaces undergoing deformation. The resulting variation in interference patterns is detected by way of phase shifts. A CCD camera is used to capture these variations and image processing techniques are used to calculate the strains. Using this method, multiple strain measurements can be done at macroscopic level.

.....

**Figure 2-7** Speckle interferometry (Saleem et al., 2005)

### LASER extensometers:

Laser extensometer is a specially designed instrument which adopts the unique laser beam technique to measure non-contact strain on materials subjected to tensile or compressive loads. Basically, the specimen surface is illuminated by laser light which when reflected is captured by a CCD camera and finally the images captured are processed by using complex algorithms. Since this device utilises the laser technology, it causes minimal damage to the specimen. They are known for high precision, high accuracy (resolution less than one micrometer) and minimal maintenance. The main advantages in using laser extensometer are as follows:

1. The use of a scan receiver on the opposite side of the specimen can be avoided since this technique applies the laser beam technique which helps in measuring the dimension changes from one side of the object;
2. It is not essential to attach marks on the specimen surface thus helps in saving time during measurements; and
3. It can be used even at elevated or sub-zero temperatures.

These devices however can measure only single strains and cannot be used for strain mapping (Hercher et al., 1987).

.....

**Figure 2-8** Laser extensometers [7] and [8]

[jolifukyu.tokai-sc.jaea.go.jp](http://jolifukyu.tokai-sc.jaea.go.jp)

[directindustry.com](http://directindustry.com)

### Photoelastic method for strain analysis:

Photoelastic phenomena may be used as a means of detecting the deformation of a substrate. An example of this method utilises a silicone (polydimethyl siloxane; PDMS) substrate, which has properties of optical retardance. A Polscope with associated computer software, which has been pre-calibrated for the specific material, is used to observe the specimen. A video of the traction – deformation is taken with the help of the polscope. Images are selected with time reference and the magnitude of the strain determined from the optical retardance values. The traction forces exerted by an individual cell, for example, are known to give rise to nanometers of retardance, which correspond to applied stresses in the range 10-12 to 10-11 N/mm<sup>2</sup> (Curtis et al. 2007).

## 2.6 DIC for non-contact strain analysis

Various non-contact optical methods, including both interferometric techniques and non-interferometric techniques, are other common methods to measure full field deformations. Among those non-contact methods, Digital image correlation (DIC), a member of non-interferometric optical technique, is considered as a flexible and a powerful tool for surface deformation measurement (Pan et al., 2009). This image analysis technique is widely used in quantification of deformation in terms of strain, and is very popular because of its relatively simple experimental setup and ease of specimen preparation. It uses ordinary white light for illumination, has a wide range of resolution and sensitivity, and is suitable for micro or nano scale strain measurements.

DIC was first developed in the 1980s by a group of researchers (Drs. Peters, Ranson and Sutton) at the University of South Carolina to measure full-field in-plane macro-scale displacements (Sutton et al., 2009). Later in 1997, DIC was used to quantify deformations in micron and nano-meter scales. DIC can be applied to measure the deformation of a wide range of materials (e.g., metals, crack growth in crystals,

biological specimens, bio-medical materials, alloys, etc.). Based on the developments involved in implementing DIC to various materials it is of 3 types: 2D DIC, 3D DIC and DVC (digital volume correlation) for measuring in-plane displacements, curved surface displacements and internal deformation of solid objects respectively.

The basic principle of DIC involves collection of digital images of the specimen obtained before and after deformation that are compared and correlated to find the changes (shifts) between them.

The merits of this technique were discussed by Pan et al. (2009) as follows:

1. Ability to quantify the deformation of various biological materials subjected to different types of loadings with great sensitivity and resolution;
2. Calculation of various mechanical parameters like young's modulus, Poisson's ratio, stress intensity etc., based on computed strain and displacement measurements; and
3. Ability to measure surface deformations from macroscopic to microscopic and even nanoscale.

Various researchers have implemented DIC to diverse specimens to analyse their deformation levels which is explained in detail in Chapter 4. For example, DIC has been adopted to analyse and investigate the deformation of two types of specimens such as ferritic steel (metal specimen) and biological specimens, including antler bone (Da Fonseca et al., 2004).

# 3 METHODOLOGY

## 3.1 Digital Image Correlation

Image analysis is a diverse field that utilises digital image processing techniques to extract meaningful data from the digital images of an object without having any contact with it. Digital image correlation which falls under this category is the process of tracking similar physical points between the consecutive images of a deforming object to extract its full field deformation or motion or shape measurements (mechanical data). A functional correlation algorithm is designed which basically compares these images and evaluates the amount of deformation.

.....

**Figure 3-1** Representation of consecutive images of a deforming subset with respect to time (Cofaru et al., 2012)

### 3.1.1 2D DIC

#### Basic Principle

Two dimensional measurement of surface deformation of a deforming object is the basic idea of the two dimensional digital image correlations. This method is the most

suitable method to measure in-plane deformation and strain of planar object surfaces (flat specimens).

A simple image of an object acquired when it is in the undeformed state (before deformation) is considered as a reference image. Another image which is acquired when the same object has undergone deformation (after deformation) is considered to be the deformed image. The fundamental concept of 2D Digital image correlation (DIC) method is to compare and correlate these two digital images obtained before and after deformation. In order to evaluate the deformation that has occurred along the surface of the material (object), the points on the reference image that has undergone deformation in the deformed image has to be tracked. This process of mapping these deformed points from the reference image to the deformed image is achieved by comparison of gray scale distribution at each point on the image.

Generally the object surface must possess a random grey level intensity distribution which gets deformed as the object surface undergoes deformation. Thus, the corresponding location of a point on the reference image possessing a specific light intensity distribution is searched in the deformed image and matched. Finally the relative position (displacement) between the images obtained before and after the deformation is obtained. Usually the images utilised in this method are divided into a number of small areas known as subsets (a group of pixels) and correlation is performed on these subset areas to quantify deformations.

.....  
**Figure 3-2** Gray-scale correlation of deformed and undeformed sub-image.

### Experimental Set-up for 2D DIC

Typical hardware set up required to carry out two-dimensional digital image correlation includes the following devices:

- a CCD or CMOS camera with high resolution to acquire images of macroscopic specimens or a CCD camera mounted in the optical path of a microscope in order to obtain images of microscopic specimens;
- specimens with a surface possessing high contrast pattern (natural or artificial speckle pattern);
- a light source to illuminate the surface of the specimen (e.g. fibre optic illuminators); and
- software into which an appropriate correlation (DIC) algorithm (that suits the application) is coded in order to compare images acquired before and after deformation, and thereby obtain 2D displacements.

.....

**Figure 3-3** Experimental set-up for 2D DIC

### 3.1.2 3D DIC

#### Basic Principle

In order to determine the three dimensional deformation of both curved and planar objects, stereoscopic vision based 3D DIC systems have been developed involving two (or more) cameras. Such system is capable of measuring the 3D deformation of the object that experiences an out-of-plane displacement or rotation. This method eliminates the major drawback of 2D DIC methods, which lack the ability to measure object deformations when it undergoes out of plane motions. This is because the 2D DIC method utilises a single camera to measure displacement fields, which leads to errors (due to magnification changes) in the obtained displacement fields when out of plane motions occurs.

3D DIC systems utilises two cameras that allow the deformation to be viewed from different directions. The 2 cameras are arranged in such a way that they focus the same object. Each camera captures an image (initial image) of the same object but they possess different views of the same object. One camera is assumed to be a master camera (camera 1) and another one is known as camera 2. The subsets in the images taken by master camera are selected and they are correlated (using 2D DIC) with the subsets of the images taken by camera 2. Thus the 3D positions corresponding to the common object point in the undeformed state is obtained by matching these subsets. This process is repeated for all subset locations in the images obtained by the cameras. It results in a dense set of 3D points that represents the initial 3D shape of the entire object focussed. The next step is to determine the deformed 3D shape of the same object (i.e. after the object undergoes deformation).



Now the 2 cameras (camera 1 and 2) were allowed to capture the images of the same object in deformed state. Then the subsets of the images obtained by camera 1 when the object was in its initial shape were selected. Image correlation is again adopted to match these subsets with the subsets of the deformed image obtained by camera 1 and 2 separately. Thus the 3D positions corresponding to the common object point in the deformed state is obtained. This process is repeated for all the subsets of the deformed images obtained by camera 1 and 2. This yields a set of 3D points representing the deformed 3D shape of the object. Finally the deformed and undeformed 3D positions of the object determined were subtracted which results in a set of 3D displacement fields.

#### Experimental Set – up for 3D DIC

- Two CCD cameras or stereo-vision based camera system (comprised of a matched pair of cameras) to acquire 3D images on a macroscopic scale or a confocal microscope (for live cells) or a scanning electron microscope (cracks, fine grains on crystals) to acquire 3D microscopic images.
- Specimens possessing a high contrast surface suitable for 3D imaging.
- Light source to illuminate the specimen surface (e.g. fluorescent or halogen lamps)
- A system software into which the DIC algorithm (with appropriate correlation criteria, interpolation scheme and sub-pixel displacement determination schemes) is coded to compare undeformed and deformed 3D images acquired and thus to obtain 3D displacements.

.....

**Figure 3-4** Experimental setup for 3D DIC [20]

[lib.znate.ru](http://lib.znate.ru)

### 3.1.3 Comparison between 2D and 3D DIC

<b>2D DIC</b>	<b>3D DIC</b>
Best suited for 2d displacement and area analysis and cannot perceive multiplane displacements.	Best suited for multi-plane displacement and volumetric analysis.
Require 2D capture devices like conventional CCD microscopes.	Require 3D capture devices like Confocal microscopes, Micro CT, electron microscopy etc
Demand lower amount of processing power and less complex image processing and interpolation algorithms.	Demand lower amount of processing power and less complex image processing and interpolation algorithms.
Demand lower amount of processing power and less complex image processing and interpolation algorithms.	Demands very high processing power and complex image processing and interpolation algorithms.
2D systems have very high accuracy with simple algorithms.	3D systems have limited accuracy with complex algorithms, as the multi-planar displacement can become very difficult to estimate precisely, even with the most complex methods of micro displacement measurements.
Can be used with 2D specimens.	Can be used with 2D or 3D specimens. When using a 2D scaffold, the depth value becomes 0.

.....

**Figure 3-5** 2D and 3D image acquisition using cameras as input devices (Heinz et al., 2010)

### 3.1.4 Assumptions in DIC

DIC converts a series of images into physical data measurements (displacements, strains, shape deformations). That is, a series of images is utilised to detect the deformation of the object. In order to achieve this target two assumptions must be employed (Sutton et al., 2008). The first assumption is that there exists a direct correspondence between points in the image and points in the object exhibiting motion. It is this assumption which makes the possibility of using image motions to quantify the displacements occurring on the object. The second assumption is that each sub-region in the reference and deformed images possesses an adequate contrast (specific light intensity pattern). Thus a specific sub-region in the reference image having a specific contrast is searched in the deformed image and they are matched accurately. This enables the process of quantification of image motions an easier one.

The DIC method cannot achieve its target when these two assumptions fail which happens when there is any discontinuity on the surface of the object (crack or hole) and when there is a loss of contrast (during loading). Sometimes a high contrast random pattern (speckle pattern) may be applied on the surface of the object to achieve accurate matching. Debonding of this pattern may lead to loss of correspondence between motion of object and motion of image.

### 3.1.5 Procedure of DIC

The methodology of performing DIC involves three basic steps: preparation of specimen and experimental set-up; acquisition and recording of images during the process of deformation; and processing of these acquired images using digital image correlation technique to obtain strain and displacement measurements. Each step is described, in turn, in the following sections.

.....

**Figure 3-6** Overall concept of DIC [21].

[lavisoin.de](http://lavisoin.de)

#### 3.1.5.1 Preparation of specimens for DIC

##### *Specimen cleaning and sterilization*

Tissue engineering scaffolds manufactured by various methods have to be sterilised before cell seeding. The most commonly being used are 70% Ethanol, Ethylene Oxide (ETO), Gamma-irradiation and a few other methods like RFGD plasma sterilization. It should be noted that Ethanol sterilization is not ideal because it does not eliminate viruses and bacterial spores completely. There is a problem of specimen shrinking after the sterilization process. Experiments conducted at University of Toronto Canada at the Institute of Biomaterials and Biomedical engineering, is suggestive that RFGD plasma sterilization is the most ideal form of sterilization when compared to the other methods, as the scaffold volume changes

and degradation characteristics seem to have been the best with this method (Holy et al., 2001).

### Application of Speckle Pattern

DIC technique requires a specimen surface that possesses a random (non-periodic or varying) intensity distribution, in order to assist accurate deformation measurement. This is achieved by creation of a high density random pattern (speckle pattern) on the specimen surface which carries information about the deformations of the specimen surface.

In general, a speckle pattern represents the light intensity pattern observed on an image plane when the surface of the specimen is illuminated by a light source. This varying intensity pattern is caused due to the interference of a number of waves possessing similar frequency but different phase and amplitude which are added together to form a resultant wave having varying intensity and amplitude. Based on the intensity information provided by these speckle patterns, subsets of reference and deformed images are matched and correlated easily. Some specimens possess a random texture naturally that could be directly utilised for correlation while some specimens lack a naturally occurring random speckle patterns on its surface. In this case, speckles are applied manually on the specimen surface which get adhered to the specimen surface and deforms along with it .These artificial speckle patterns are generated either by spraying paints (black or white paints) or by holding the paint can at a distance such that a random gray scale pattern is established on the surface of specimen. In scaffolds speckle pattern is created by embedding random fluorescent beads, so that they form high contrast markers for image correlation (Huang et al., 2010).

.....  
**Figure 3-7** Randomly distributed fluorescent particles inside a reference subset are automatically identified and marked as a series of rectangular windows (Huang et al., 2010).

Lecompte and co-workers (2007) detected the influence of speckle patterns on displacement measurements (in-plane displacements) in the DIC technique by employing four speckle patterns (three of them exhibiting the same speckle pattern with different zoom and one with large speckles with sharp focus) with different speckle sizes and spectral content. A numerically controlled deformation was applied to these speckle pattern images and it was analysed that speckles of medium size exhibiting a limited spectral content results in more accurate displacements. The same group carried out a similar analysis by examining three speckles pattern (of different zoom levels) under two types of deformations; homogenous and heterogeneous (Lecompte et al., 2006). In both cases, speckle patterns were created by a random spray of black paint (even distribution maintained) on a flat white surface. Thus these analyses demonstrate the influence of selection of speckle size and subset size on accuracy of measure displacements which ensures the significance of speckle patterns in DIC technique.

Speckle patterning methods employed to a variety of specimens in DIC (from macroscale to microscale) are discussed in this section. Lauret et al. (2009) applied a fine random pattern (average diameter of the dots in the pattern was 0.5mm) on the brain slices by using a resin (matt black enamel) and an airbrush in order to detect strain fields on it. A fine pattern was generated by application of fluorescent silica

nanoparticles on the surface of a three dimensional microvascular network by Hamilton and co-workers (Hamilton et al., 2009 ) in order to measure strain concentrations on it using (fluorescent DIC). Sztefek et al. (2010 ), on the other hand, coated the whole periosteal surface of tibia with a thin layer of water based white paint and then it was speckled with black paint by using a high precision airbrush in order to measure surface strains on it. Speckle pattern was created by (Sutton et al., 2008) by application of toner powder (particle size 3-10 micrometers) on the mice carotid arteries and thus measured the surface strain fields. White paint spray followed by black paint spray over this white background on a transverse weld tensile specimen formed a high contrast speckle pattern which assisted in determining its mechanical behaviour (Reynolds et al., 1999). A similar speckle patterning method was applied to pure titanium sample surface (Toussaint et al., 2008) and cylindrical aluminium block surface (Tong, 2004) in order to detect strain fields on them.

.....

**Figure 3-8** A typical speckle pattern [9]

[cranfield.ac.uk](http://cranfield.ac.uk)

.....

**Figure 3-9** Speckle pattern on aortic specimen used for DIC analysis [10]

[ul.ie](http://ul.ie)



### 3.1.5.2 Image Acquisition

The first stage of any vision system is the stage of image acquisition. After the image has been acquired, various methods of processing can be applied to the image to perform the many different vision tasks required today. However, if the image has not been acquired satisfactorily then the intended tasks may not be achievable, even with the aid of some form of image enhancement.

#### 2D Image Acquisition

The images thus obtained, used for 2D DIC represent a 2D projection of the surface of the specimen. To obtain an image of the required physical point on the specimen surface and to obtain accurate displacement, the following conditions have to be met:

- the surface of the specimen or scaffold has to be flat, i.e., the object surface should be parallel to the CCD sensor;
- out of plane displacements should be avoided, since it may lead to magnification of the recorded images, which further leads to inclusion of additional in-plane displacements; and
- geometric distortions that include additional displacements due to the loss of linear correspondence between physical point and imaging point should be removed.

Generally modern scientific grade digital cameras such as CCD (charge coupled device) and CMOS (complementary metal oxide semi-conductor) cameras, coupled to the optics of a microscope are used for deformation measurement based on image correlation. CCD cameras were widely used since 1970s for image analysis applications. Later as the manufacturing technology has advanced CMOS cameras were introduced and used for this purpose. Eventhough these cameras had many advantages like availability of more chip functions, lower power dissipation (at chip level), smaller size they faced many drawbacks such as reduced image quality and flexibility. Thus these cameras are used in 2D DIC to obtain high quality images of the specimen surface on the sensor plane and transfer these digital data obtained in the form of intensity at each sensor location to a proper storage location.

.....  
**Figures 3-10** CCD AND CMOS cameras [11]

[news.directindustry.com](http://news.directindustry.com)

*2D and Stereo Microscopy with Image Correlation and Processing*

2D and stereo microscopy with image correlation and processing is a real-time image acquisition system which makes use of a CCD Camera coupled system. By far the most popular two-dimensional imaging device is the charge-coupled device (CCD) camera. This is a single IC device, consisting of an array of photosensitive cells. Each cell produces an electric current dependent on the incident light falling on it. So, there is a video Signal output at a frame rate depending on the type of CCD used. There is less geometric distortion and a linear video output.

.....

**Figure 3-11** Stereo microscope coupled with digital camera system [12]

[olympusmicro.com](http://olympusmicro.com)

### 3d Image Acquisition

#### Micro CT 3D Structure Analysis

Computerised Tomography (CT) is a macroscopic 3D scanning system used in medical diagnostics and industrial research. They make use of X-Rays and a detector to create 2D cross sectional images of the 3D object, which are later rendered into 3D point clouds and nodes by 3D rendering softwares. In the conventional CT system, the detector and the X-ray emitter rotate around the object. This system has resolutions nearing 2 mm.

A microCT system, as the name suggests, has higher resolutions and is built for minuscule scanning applications. In this setup, usually the sample rotates and the scanning setup is stationary. This setup is usually used to analyse small laboratory samples, insects and small animals. They have a very good 3D resolution but have radiation exposure hazards similar to the large scale CT scanners.

.....  
**Figure 3-12** Micro CT scanner [13] and [14]

[mayoresearch.mayo.edu](http://mayoresearch.mayo.edu)      [skyscan.be](http://skyscan.be)

### Electron Microscopy

Electron microscope is a form of microscope which uses electrons striking a phosphor plate to create images. This system is capable of higher magnification and greater resolution, as it has a lower wavelength when compared to visible light. Though this has many advantages, it is a very expensive piece of equipment and requires frequent maintenance of parts and highly trained technicians. The images obtained are 2D but can be reconstructed using specialized algorithms to 3D. There are also 3D scanning electron microscopes, in which the electron take a curved path around the object to be magnified and the amount of deflection is reconstructed into a 3D image. The electron microscopes with such capabilities are also known as 3D (Electron Tomography). One of the main disadvantages of the system being that it operates under vacuum and live biological tissue cannot survive that kind of temperatures. Also the electron beam can kill any live cells in its field.

.....  
**Figure 3-13** Electron microscope [15] and [16]

[purdue.edu](http://purdue.edu)

[labx.com](http://labx.com)

*Confocal Microscopy – 3D Real-time and Recorded*

The concept of confocal imaging was patented in the year 1957. The confocal microscope overcomes some disadvantages of conventional wide field microscopes. In the conventional microscopes, also known as ‘wide field’ microscopes, the specimen is beamed with light entirely and all the parts of the specimen are made to be fluorescent at the same time and this fluorescent glow is detected by the cameras. In contrast to the wide field microscopes, the ‘confocal’ use point- illumination techniques. The point focussed on the focal plane can only be detected by the detector, meaning the microscope can have depth perception as well. However, the time taken for the entire image to be scanned as a point cloud is much longer than in any microscopes and hence live images cannot be acquired. The thickness of the focal plane is derived numerically by dividing the wavelength of the lens by the focal length of the lens. This microscope is good at 3D imaging and hence can be used to find precise texture of surfaces even without contact, unlike Atomic Force Microscopes (AFM) which require physical contact.

.....  
**Figure 3-14** Confocal microscope [17] and [18]

[olympusamerica.com](http://olympusamerica.com)

[med.unc.edu](http://med.unc.edu)

Because of the complexity and lack of feasibility of the other methods discussed, and the use of 2D scaffolds for strain measurements, the discussion here is restricted to the use of 2D DIC for strain measurement.

### 3.1.5.3 Image Pre-processing

#### *Image Registration*

Image registration is defined as “the mapping of images with respect to spatial domain and intensity in order to estimate the optimal transformation between the images” (Brown, 1992).

### Need For Image Registration

The DIC technique involves the comparison (pixel by pixel comparison) of consecutive images of the deforming specimen by establishing point-to-point correspondence between these images. In order to achieve this level of correspondence, these images must be spatially registered, i.e., the acquired images are overlaid (spatially aligned) upon one another thus enabling common features in those images to get aligned with one another. As a result, all the images are obtained in the same reference co-ordinate system, which assists in correlation process (performed by DIC). Thus image registration is the method of pre-processing the images acquired before carrying out correlation process (DIC).

### Steps Involved In Registering An Image

According to this method, two images are considered, of which one is called as the reference or source image and the other is called the sensed or target image. Each and every corresponding point of these pairs of images are detected and matched such that the transformation existing between each point is determined. For this purpose, the reference image is kept unchanged and the sensed image is transformed to take the spatial co-ordinates of the reference image. The article by Zitova et al. (2003) describes the four most important steps followed during image registration. These are:

- *Feature Extraction:*  
The distinct features (such as shape of the object, boundaries surrounding a region, lines, points etc.) in both reference and sensed images are detected and selected.
- *Feature Matching:*  
A correspondence is determined between the selected features in both reference and sensed images.
- *Transform Model Estimation : (or Transformation Function Determination)*  
Both reference and sensed images were aligned and the parameters of mapping functions (transformation parameters) were determined with the help of corresponding feature points detected in the last step.
- *Image Resampling and Transformation:*

The sensed image is resampled and transformed to the geometry of the reference image using the transformation functions.

#### Intensity-based Vs Feature-based Image Registration

Depending upon the technique used for registering an image, image registration or image alignment methods are classified into two types. They are intensity based image registration and feature based image registration. Intensity based image registration methods works normally by comparing the intensity patterns between the images while feature based image registration methods works by detecting the correspondence between a number of distinct points (features like points, lines and contours) between images. In general, intensity based registration methods lack specificity while feature based registration methods are more specific. In terms of sensitivity, feature based image registration methods are less sensitive than the intensity based image registration methods. Hence, in order to achieve best registration, it is desirable to make use of both the registration methods in a combined form. By doing this, both the properties specificity and sensitivity are balanced.

#### 3.1.5.4 Image Processing (Image correlation)

##### Basic Concepts

##### Correlation Criteria

As discussed under section 3.1.1, a subset (comprising a group of pixels) chosen from the reference image has to be searched and located among the various subsets of the deformed image on the basis of gray intensity distribution of these subsets. Thus it is necessary to evaluate the similarity degree between the subsets of reference and deformed images in order to track the correspondence and evaluate the displacements between them. Practically a correlation function is usually predefined to evaluate this similarity. When the peak position of the distribution of this correlation co-efficient is searched and detected, the matching procedure (detection of similarity) is completed. A basic correlation function is defined as,



$$\text{COF} = \frac{\sum G_{ij}G_{IJ}}{\sqrt{\sum G_{ij}^2 \cdot \sum G_{IJ}^2}}$$

Where  $G_{ij}$  is the gray scale of reference subset (undeformed subset) on co-ordinates (i, j) and  $G_{IJ}$  is the gray scale of deformed subset on the co-ordinates (I, J) respectively. When there is an exact correspondence between the undeformed and deformed subset (i.e., when the difference between the grayscale intensities of reference and deformed subset is zero), this co-efficient becomes equal to 1. Thus the subset from the reference image is perfectly tracked and located in the deformed image. But this does not happen often because the gray level intensity of the deformed subset varies with that of the reference subset in most cases which may in turn lead to an intensity mismatch between them. This mismatch can be corrected by improving the design of the correlation criterion adopted. Thus the target of a good correlation criterion must be to minimise the difference in the grayscale intensity between the reference and deformed subsets. In order to avoid this, a robust correlation criterion has to be established. Pan (2011) identifies four categories of correlation criteria used in DIC. They are: cross correlation criterion (CC); sum of absolute difference (SAD) criterion; sum of squared difference (SSD) criterion; and parametric sum of squared difference (PSSD) criterion. Tables 1 and 2 (below) give the definitions and performance of each correlation criteria.

Even when the process of image acquisition (in either 2D DIC or 3D DIC) is carried out under ideal conditions, there are many circumstances which lead to inaccurate correspondence (mismatch) between the reference and deformed subsets. One such circumstance is significant changes in the intensity values of the images acquired. These intensity changes are due to several reasons like disturbances in lighting, orientation of specimen and reflection from specimen surface (during experimentation), which does not influence the entire image, i.e., changes are localised. This problem of intensity changes is very common when stereo image subsets were matched. This is because the same object has been viewed at different angles by the 2 cameras used.

In order to compensate the errors caused due to these intensity changes; the correlation criteria used usually should be optimised. This lead to the derivation of normalised (NCC, NSSD, NSAD), zero mean (ZCC, ZSAD, ZSSD) and zero-mean normalised (ZNCC, ZNSAD, ZNSSD) correlation criteria, which are adopted and suggested by Sutton et al. (2009), Pan et al. (2009) and Pan (2011), in order to compensate for offset and scale changes in lighting. The more common CC, SAD and SSD correlation criteria are sensitive to all lighting changes and hence rarely used. The ZCC, ZSAD, ZSSD correlation criteria are insensitive to offset changes of lighting but sensitive to scale changes of lighting while NCC, NSAD, NSSD correlation criteria are insensitive to scale changes of lighting but sensitive to offset changes of lighting. The ZNCC, ZNSAD and ZNSSD correlation criteria are the more robust, being relatively insensitive to fluctuations in lighting (both offset and scale changes).

It is difficult to control the changes in lighting in practice, however. Thus the optimised correlation criteria discussed above offer a practical solution to obtain a higher rate of correspondence between the reference and deformed subsets even in the presence of localised intensity changes within the acquired images.

<b>CORRELATION CRITERION (CC)</b>	
Cross-correlation (CC)	$C_{CC} = \sum_{i=-M}^M \sum_{j=-M}^M [f(x_i, y_j)g(x'_i, y'_j)]$
Normalized cross correlation (NCC)	$C_{NCC} = \sum_{i=-M}^M \sum_{j=-M}^M \left[ \frac{f(x_i, y_j)g(x'_i, y'_j)}{f' g'} \right]$
Zero-normalized cross-correlation (ZNCC)	$C_{ZNCC} = \sum_{i=-M}^M \sum_{j=-M}^M \left\{ \frac{[f(x_i, y_j) - f_m] \times [g(x'_i, y'_j) - g_m]}{\Delta f \Delta g} \right\}$
<b>SUM OF SQUARED DIFFERENCES CORRELATION CRITERION</b>	
Sum of squared difference (SSD)	$C_{SSD} = \sum_{i=-M}^M \sum_{j=-M}^M [f(x_i, y_j) - g(x'_i, y'_j)]^2$
Normalized sum of squared differences (NSSD)	$C_{NSSD} = \sum_{i=-M}^M \sum_{j=-M}^M \left[ \frac{f(x_i, y_j)}{f'} - \frac{g(x'_i, y'_j)}{g'} \right]^2$
Zero-normalized sum of squared differences (ZNSSD)	$C_{ZNSSD} = \sum_{i=-M}^M \sum_{j=-M}^M \left[ \frac{f(x_i, y_j) - f_m}{\Delta f} - \frac{g(x'_i, y'_j) - g_m}{\Delta g} \right]^2$

**Table 1** Commonly used correlation criteria [redrawn from (Pan et al., 2009)].

Where,

$$\Delta f = \sqrt{\sum_{i=-M}^M \sum_{j=-M}^M [f(x_i, y_j) - f_m]^2}$$

$$\Delta g = \sqrt{\sum_{i=-M}^M \sum_{j=-M}^M [g(x'_i, y'_j) - g_m]^2}$$

$$f_m = \frac{1}{(2M + 1)^2} \sum_{i=-M}^M \sum_{j=-M}^M f(x_i, y_j)$$

$$g_m = \frac{1}{(2M+1)^2} \sum_{i=-M}^M \sum_{j=-M}^M g(x'_i, y'_j)$$

$$f' = \sqrt{\sum_{i=-M}^M \sum_{j=-M}^M [f(x_i, y_j)]^2}$$

$$g' = \sqrt{\sum_{i=-M}^M \sum_{j=-M}^M [g(x'_i, y'_j)]^2}$$

PERFORMANCE	CC CRITERIA	SAD CRITERIA	SSD CRITERIA
Sensitive to all changes of the deformed subset intensity	$C_{CC} = \sum f_i g_i$	$C_{SAD} = \sum \text{mod}(f_i - g_i)$	$C_{SSD} = \sum (f_i - g_i)^2$
Insensitive to offset changes of the deformed subset intensity	$C_{ZCC} = \sum (f'_i g'_i)$	$C_{ZSAD} = \sum \text{mod}(f'_i - g'_i)$	$C_{ZSSD} = \sum (f'_i - g'_i)^2$
Insensitive to scale changes of the deformed subset intensity	$C_{NCC} = \frac{\sum f_i g_i}{\sqrt{\sum f_i^2 \sum g_i^2}}$	$C_{NSAD} = \text{mod}\left[\frac{f_i}{\sqrt{\sum f_i^2}} - \frac{g_i}{\sqrt{\sum g_i^2}}\right]$	$C_{NSSD} = \sum \left[\frac{f_i}{\sqrt{\sum f_i^2}} - \frac{g_i}{\sqrt{\sum g_i^2}}\right]^2$
Insensitive to the scale and offset changes of the deformed subset intensity	$C_{ZNCC} = \frac{\sum f'_i g'_i}{\sqrt{\sum f_i'^2 \sum g_i'^2}}$	$C_{ZNSAD} = \text{mod}\left[\frac{f'_i}{\sqrt{\sum f_i'^2}} - \frac{g'_i}{\sqrt{\sum g_i'^2}}\right]$	$C_{ZNSSD} = \sum \left[\frac{f'_i}{\sqrt{\sum f_i'^2}} - \frac{g'_i}{\sqrt{\sum g_i'^2}}\right]^2$

**Table 2** Correlation criteria used in DIC to evaluate the similarity degree between the reference subset and deformed subset [redrawn from (Pan, 2011)].

Where,

$$f' = \frac{1}{n} \sum_{i=1}^n f_i$$

$$g' = \frac{1}{n} \sum_{i=1}^n g_i$$

$$f'_i = f_i - f'$$

$$g'_i = g_i - g'$$

$f(x_i, y_j)$  and  $g(x'_i, y'_j)$  denote the gray values of the  $i^{\text{th}}$  pixel of the reference subset and the target subset.

#### Interpolation Scheme

An image comprises a discrete set of points (pixels) each representing a specific amount of light intensity. Searching and tracking a specific point (possessing a specific light intensity) that belongs to the reference image in the deformed image is quite difficult. This is because, non-integer displacements were introduced in the deformed images corresponding to similar positions in the reference image, i.e., intensity values lying at integer positions, in terms of pixel level, in the reference image could be found only at non-integer positions (sub-pixel level) of the deformed image due to the deformation of the object which is imaged. Thus sub-pixel level image comparison (between the reference and deformed images) becomes mandatory to extract accurate displacements. Thus, the undeformed and deformed images used for correlation (DIC) should possess a high resolution in order to carry out sub-pixel based comparisons. Here arises the importance of using an interpolation scheme to satisfy this requirement.

Interpolation is nothing but introduction of probable data using the known data available, that is, estimation of a new unknown pixel value in an image by utilizing the neighbouring known pixel values. This process is utilised in image processing to obtain an image with a high resolution. In other words, the available data samples (known pixels in an image) are smoothed by introduction of acceptable intermediate

data (interpolated pixel) between them, and, in this way, an image with the best approximation of its intensity and colour can be achieved. Higher order interpolations are implemented in digital image correlation algorithms to carry out sub-pixel based comparisons between the undeformed and deformed images and thus displacement and strain results with sub-pixel accuracy are obtained.

Prajapati et al., (2012) and Htwe (2010) described the classification of interpolation which is of two types: adaptive and non-adaptive. As the name suggests, adaptive interpolation algorithms adapt themselves according to the characteristics of the image, in terms of the texture of the image, for example (irrespective of whether it is sharp or smooth). Thus, these algorithms are sensitive to the changes within each pixel of the image and thus all the pixels are not treated equally, hence the approach of processing varies for each pixel. They help in estimating the lost pixel values in an image by utilizing the features of adjacent pixel values. Thus these algorithms involve complex calculations and are often used to minimise interpolation artifacts (for example, edge halos, blurring, and/or aliasing) in the enlarged images. Non-adaptive interpolation algorithms follow a fixed pattern of computation which is very simple compared to adaptive type. Here, each and every pixel in the image is treated equally. Thus, in short, computational logic of adaptive interpolation algorithms depends on the content of the input image (input features) whereas non-adaptive type works independently irrespective of input image content.

Examples of non – adaptive interpolation algorithms includes nearest neighbour, bi-linear, bi-cubic, spline , sinc, lancos and median interpolation. Non-adaptive interpolation methods usually use adjacent pixels for interpolation. Depending on the number of adjacent pixels used for interpolation, these are classified as: nearest neighbour, bi-linear and bi-cubic type. Nearest-neighbour interpolation is the simplest type in which the nearest (adjacent or closest) pixel is used to fill the interpolated point. This method of interpolation effectively increases the size of each pixel since the values of nearest pixel is simply copied (no change in pixel values). An important merit of this interpolation is that image processing is fast (requires less processing time). Bilinear interpolation method fills the interpolated point (unknown pixel value) with weighted average of surrounding four known pixel values

considered closest across  $2 \times 2$  matrix positions within an image. Thus as the name indicates, two linear interpolations are handled (horizontal and vertical directions) and the distances between known pixels and interpolated pixels are equal. Median interpolation determines the interpolated pixel value by calculating the median of four nearest pixels surrounding it. Eventhough it offers better results than nearest neighbour and bilinear interpolations it causes image blurring which cannot be avoided.

Bi-cubic interpolation fills the interpolated point with the weighted average of surrounding known sixteen pixel values considered closest across  $4 \times 4$  matrix positions within an image. In this case the known pixels are not at an equal distances from the unknown interpolated pixel and pixels of more proximity are given higher importance during calculations. Of these three methods, bi-cubic method offers better resolution (smooth) images with high quality due to which they are commonly adopted for DIC applications. Spline and sinc are higher order interpolations which consider more number of surrounding pixels in order to fill the interpolated point. Thus their computation logic is very intense and requires long processing time.

Since images are changed from one resolution to another resolution during interpolation, obviously there occurs certain artefact which cannot be avoided but can be reduced. Non-adaptive interpolation methods cannot eliminate the artifacts completely but they have the capability to balance the levels of artifacts occurring within images during interpolations. Adaptive interpolation methods in contrast will not produce such artifacts but they may introduce strange pixels in between which may or may not assist the image enhancement.

.....  
**Figure 3-15** Interpolation schemes a. Bi-cubic interpolation b. Bi-linear interpolation [19]

[cambridgeincolour.com](http://cambridgeincolour.com)

.....  
**Figure 3-16** Gray scale interpolation

.....  
**Figure 3-17** RGB interpolation – comparison of non-adaptive interpolation methods (Prajapati et al., 2012)



#### Sub-Pixel Displacement Registration Algorithms

Sub-Pixel registration algorithms are important when high precision is required in Digital Image Correlation based measurements. Such algorithms work similar to interpolation schemes by estimating the values between the integer pixels and thus improve the correlation peak of DIC. Several Sub pixel registration schemes have been used (Bing et al., 2006; Pan et al., 2009; and Xiong et al., 2011), but it is to be noted that with increasing complexity of such algorithms, there is a proportional increase in processing load. Hence the increase in precision of DIC measurements using Sub-Pixel algorithms comes at the cost of processing speed. So the use of Sub-pixel algorithms should be justified based on the application and the amount of precision required.

#### 3.1.5.5 Image Post Processing

##### Displacement Measurement

The square reference subsets are chosen from the reference image and its corresponding location is tracked in the deformed image. A square subset is often used for comparison rather than a pixel because; a subset possesses a group of pixels and thus exhibits a wide variation in gray levels (light intensity). This intensity variation within the subset allows it to distinguish from other subsets. Thus the targeted subsets (chosen from the reference image) can be easily identified in the deformed image. After locating the targeted subset, similarity between the reference image subset and the deformed image subset is evaluated by adopting two types of criteria, namely, the cross-correlation (CC) criterion and sum-squared difference criterion. This is followed by searching of peak position of the distribution of correlation co-efficient. Finally, the displacement vector is found by calculating the difference between the reference subset centre and target subset centre (in the deformed image).

.....  
**Figure 3-18** Concept of displacement measurement in DIC (Tang et al., 2012).

*In – Plane Displacements – Adoption of 2D DIC*

2D scaffolds, lead to cell attachment in such a way that there cannot be traction forces in any other planes. Hence, when such scaffolds are used, the displacement measurements are fairly straightforward and the 2D DIC can be used with high amount of precision. The precision can be improved by using a better CCD or CMOS sensor in the microscope or by using sub-pixel interpolation methods for both image registration and correlation.

*Out of Plane Displacements – Adoption of 3D DIC*

Many futuristic research methods focus on creating on an environment for the cell, which would stimulate its physiological conditions inside the biological environment, where there are traction forces in multiple directions and different planes. Hence, if 2D techniques are used, there can be a number of measurement errors, as they cannot visualise the out of plane measurements and consider them to be located in the same plane. 3D DIC techniques have to be used in these conditions to identify volumetric changes caused by cell traction forces and displacements caused in multiple planes.

### Strain Measurement

#### Strain Mapping

Strain is a basic physical entity which represents a relative ratio of displacement between any two points on an object to the reference length of the object. Since it helps to quantify the amount of deformation of any object subjected to stress, it greatly assists in deciding the mechanical strength of the object. DIC is implemented in this review to measure local 2D displacements of a tissue engineered scaffold. Later these measured displacements (known data) and the reference length of the scaffold (known data) are used to measure local strains of the scaffold. Local displacement and local strain indicates the amount of displacement and strain experienced by the scaffold at each and every point on its surface, that is, at each and every subset of the scaffold images used in DIC. Thus by technically measuring strain on a scaffold, it assists tissue engineers in designing a scaffold with better tissue formation characteristics.

To explain the concept of measuring strain on a 2D scaffold surface, let us consider two images (undeformed and deformed images) of the scaffold surface. It has been already discussed that the images are sub-divided into smaller and similar sized square sections known as subsets to carry out DIC. Each subset of the undeformed image with dimensions  $dx * dy$  is a perfect square and the corresponding subset of the deformed image tracked using DIC concept takes a rhombus form due to deformation. The displacement of the subset is given as,

.....

Figure 3-19 Strain measurement concept in DIC (Tang et al., 2010).

**Displacement in x dimension =  $Dx = x' - x$  ..... 1**

**Displacement in y dimension =  $Dy = y' - y$  ..... 2**

Thus the displacement of the subset considered on the scaffold surface is given by,

**Displacement of the subset =  $Ds = \sqrt{(x' - x)^2 + (y' - y)^2}$ ..... 3**

The strain experienced by the subset considered is given by,

**Strain of the subset =  $Sb = \frac{Ds}{L} = \frac{\sqrt{(x' - x)^2 + (y' - y)^2}}{L}$  ..... 4**

**Reference length =  $L = \sqrt{(x - x^0)^2 + (y - y^0)^2}$  ..... 5**

Where  $(x^0, y^0)$  represents the origin.

Thus the displacement and strain is calculated for every subset (local regions) in the images. These local strains and displacements are plotted in a map which is named as strain map and displacement map respectively. Both these are almost similar. The

strain map is plotted in such a way that each range of strain level is indicated by a specific colour. These maps aid in deformation analysis, that is, one can predict the areas of the scaffold which has undergone larger or medium or smaller deformation for a given amount of stress applied on it. Strain maps can be plotted either of the two ways, 2D or 3D. 2D strain map is a plot of local strains on the scaffold surface while a 3D strain map is a plot of local strains of the entire scaffold (3D surfaces). 3D strain maps indicate the amount of deformation by peaks.

Strain and displacement maps allow one to analyse the distribution pattern of deformation throughout the scaffold area that is subjected to an applied stress (created by cells seeded on the scaffold) whether or not it is of homogenous or heterogeneous distribution. When this distribution pattern almost matches the ECM, then the scaffold is considered to exhibit better tissue formation characteristics.

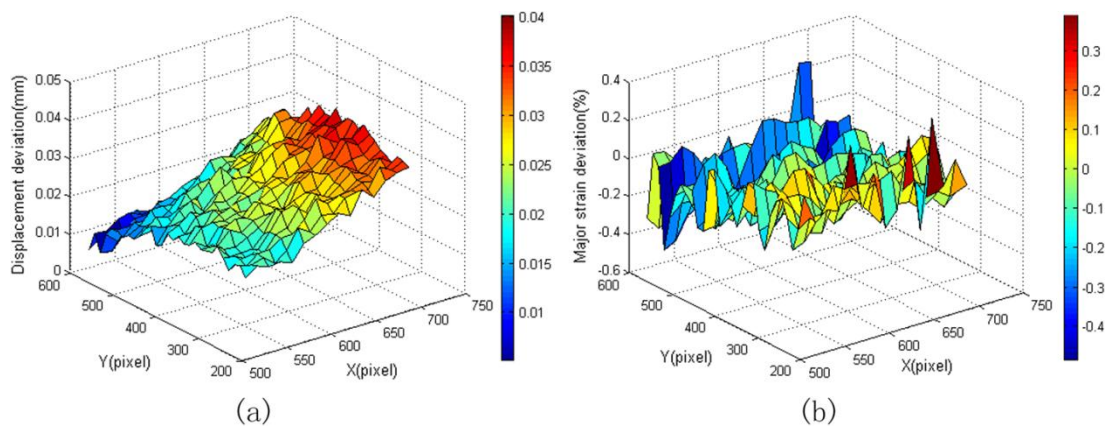


**Figure 3-20** (a) 3D displacement map (b) 3D strain map



**Figure 3-21** Process of scaffold evaluation using digital image correlation

## 4 IMPLEMENTATION OF DIC

Since DIC technique works only on the images of the surface of the specimen acquired, it usually has diverse applications irrespective of the specimen size. Thus DIC find its applications right from large structures (bridges, aeroplanes) to micro or nano sized structures (cells, crack growth, grain sized particles) obtained with the help of optical or electron microscopy. Thus DIC implementations on macroscale and microscale specimens have been discussed in this section.

### 4.1 Macroscale Implementation

#### 4.1.1 On Biological Specimens (On Bones)

##### Measurement Of Strains In Cartilage:

Wang et al., (2002) implemented an automated approach in order to measure 2D strain distribution in the cartilage specimen (carpometacarpal joint cartilage) subjected to unconfined compression. This approach is a combination of various techniques (video microscopy, optimised DIC, thin plate spline smoothing (TPSS), generalised cross validation (GCV)) among which optimised DIC technique has been validated as an important one for cartilage mechanics application. Three important schemes have been adopted under this optimised DIC technique order to measure the displacements and improve the displacement accuracy. They are bi-cubic spline interpolation scheme, quasi Newton algorithm and normalised correlation criteria. Chondrocytes within cartilage and their nuclei were fluorescently labelled and when they were seen under the condensed transmission light (from the microscope), the relative position between the cells (or cell nuclei) results in a random pattern on the sample surface which is a basic criteria to enable image correlation.

##### Measurement of Strains in Mandible:

Tanasic et al. (2012) presented the DIC method as an appropriate method to determine strain distribution of structures with complex geometry (mandible surface used here). The removable and partial dentures (prosthetic replacements) were placed on the posterior mandible bone (dried mandible with shortened dental arch used

here) and were subjected to a loading of 50-300 N. A high contrast surface of the replacements and the specimen mandatory to perform DIC were obtained by coating their surfaces with a thin white layer and a black paint (spraying method). After loading, the corresponding strains (during loading) on the mandible surface and the replacements were evaluated using DIC technique. 2 digital cameras and the Software ARAMIS which is capable of measuring and analyzing 3D strain distributions under static and dynamic loading were used to perform 3D DIC.

#### Measurement of Surface Strains on Tibia:

Sztefek and co-workers (Sztefek et al., 2010) estimated bone surface strain by subjecting the murine tibia (of mouse) specimens to compressive loading. The specimen surface was coated with a thin layer of white and black (acrylic water based) using a high precision airbrush to obtain a high contrast speckle pattern. Images of specimen surface were acquired using 2 digital cameras which were processed (3D DIC strain analysis) using ARAMIS (1.3 M system) software. It has been found that non-uniform tensile strains and compressive strains were formed along the medial side and lateral sides of the mouse tibia respectively during loading. Later when the bone was allowed to undergo an adaption for a period of two weeks, it was found to exhibit uniform strain along the medial side after adaption. Thus utility of DIC technique has enabled a clear perception about the mechanism of adaption of a bone to a mechanical load and the effects of adaptive changes inside a bone due to the surface strains.

#### Use of Strain in Bone Tissue to Detect Fractures:

Micropores and micro-cracks caused due to the strain fields in the bone is a potential cause for its fracture. Thus it is quite essential to understand the relationship between micro-crack development and strain distribution in bone tissue. The study by Yamaguchi et al., (2011) explains this relationship by analysing the strain distribution on bone tissue surface using image correlation techniques (DIC). Micro-cracks developed during a 3-point bending fracture toughness test on a bovine cortical bone of femoral shaft were recorded using a high speed camera. Strain distribution was measured using DIC technique. An image obtained before and after



deformation is compared on the basis of pixel luminance values. In order to minimise the time consumed for analysis a detailed search was performed between the sub-pixels of the subset (a small portion of an image). Under this search, luminance values of the corresponding sub-pixels were obtained by using bi-cubic interpolation scheme. This experiment was conducted even when the bone is preserved in 3 different types of storage solutions like neutral buffered formalin, ethanol, and saline solution to analyse the bone surface strain analysis.

#### Measurement of Strain on a Fresh Bone:

Bland and co-workers (Bland et al., 2010) performed an investigation on the characterization of a fresh bone using stereo DIC. Chicken tibia specimens were subjected to load with the help of a setup that applies force on these specimens both axially and transversely. After loading, SDIC (stereo DIC) has been employed to determine the 3D surface strain distribution and mechanical properties (elastic modulus) of these fresh bone specimens immersed in a phosphate buffered saline (PBS) solution. It has been noted that the strain distribution is quite different for bones loaded axially and transversely. Later the specimens were removed from the solution and dried in order to detect the change in strain distribution (compared to strain distribution of immersed bone) under this condition (as the drying time increases). Finally it has been proved that the strain distribution obtained for an immersed bone almost mimics the strain distribution of a bone under in vivo condition thus enabling to characterise its exact mechanical properties.

## 4.2 Microscale Implementation

### 4.2.1 On Biological Tissues

#### Detection of Mechanical Behaviour of Arterial and Hard Tissues:

The application of DIC on biological tissues has been demonstrated in a study by Zhang et al., (2004), in which the mechanical behaviour of tissues (elastic modulus and Poisson's ratio of the specimens were calculated and compared) such as bovine artery and bovine hoof horn were investigated. Appropriate surface preparation

methods (paint spray method) were handled to obtain a typical (high contrast) speckle pattern of the hydrated tissue surface. Uni-axial tension experiments were conducted on these specimens and their corresponding surface strains and displacements were calculated with sub-pixel accuracy by implementing the fast search strategy, “Newton Raphson Scheme”. The strain distributions and stress strain response of arterial wall (arterial tissues) and wet cow hoof horn (dermal tissues) were analysed.

#### Validation of Incompressibility of Brain Tissues:

3D DIC has been utilised to validate the incompressibility of the brain tissue by Libertiaux et al., (2011). Tissue samples used for testing were applied with a suitable speckle pattern (three step process) for proper imaging and direct application of DIC such that they do not cause any significant changes to the mechanical properties of the tissue. Three types of tests such as unconfined compression tests, relaxation tests and cyclic tests were performed on cylindrical samples of swine brains using DIC in order to evaluate the deformed geometry (strains) of these samples and determine their volumes(volume ratios) which are shown below. Three stereoscopic systems comprising of 6 CCD cameras were used for imaging the 3D shape of the sample surface. An optimised correlation co-efficient is used to achieve a good correspondence between the deformed and undeformed image pairs.

#### Deformation Measurement of Skin Tissues:

DIC in combination with finite element modelling has been proved as an excellent method to characterise the in-vivo deformation of skin by Evans and Holt (2009). A model (finite element model) that resembles the characteristics of the real skin (Ogden hyperelastic membrane) has been used to optimise the material properties. This model was solved iteratively until the deformation data obtained from the model matches with the similar data obtained with the help of DIC.

### Deformation Measurement of Soft Tissues:

Tissues (soft tissues) subjected to dynamic loading (during practical body injuries) experience non-equilibrium and high strain rate deformations and it is difficult to measure the tissue response due to these deformations with the help of traditional mechanical testing methods. Mates and co-workers (Mates et al., 2009) utilised a 3D DIC that comprised high-speed stereo imaging camera pairs (capable of recording 180,000 frames per second) to measure such deformations.

### Detection of Tissue Deformations Subjected to Diagnostic Insertions:

Percutaneous intervention which involves the insertion of certain instruments (catheters or probes or needles) into the soft tissues of our body in order to reach the internal target organs is an important process followed to carry out many diagnostic procedures. But at times inaccurate insertions (target movement or probe deflection) may occur due to the deformation or inhomogeneity property of the target tissues. Thus it is necessary to study the tissue behaviour (soft tissue deformations) during such insertions. Kerl and colleagues (Kerl et al., 2012) adopted a laser-based digital image correlation method to determine such deformation. Gelatin samples that mimic the soft tissue samples were inserted with a needle probe to cause deformations on it. Micrometer sized particles embedded on the samples (during sample preparation) undergoes displacements during insertion process. These movement pattern is tracked and imaged (using a CCD camera) when these particles were illuminated by a thin laser light. This process is repeated for various time delays after which the cross correlation DIC algorithms were used to compare the sub-regions of the images and hence the displacements are calculated.

### Measurement of Strain Concentrations around Tumour:

Basal cell carcinoma is a type of skin cancer caused due to high exposure to UV light. Development of lesions due to BCC interrupts the normal functioning of surrounding tissues. Patients requiring BCC removal were recommended for a standard surgical resection or Moh's microscopic surgery. In order to remove tumour with standard surgical resection borders of BCC (margins of tumour) should be

identified. When the skin is stretched, strain gets concentrated within tumour. It is these strain concentrations that helps in identification of tumour borders. Krehbiel et al., (2010) employed a DIC technique to evaluate these strain concentrations. A coarse fine search coupled with Newton Raphson scheme based DIC code was used to measure accurate displacements and strains. DIC has been suggested as a rapid technique to identify the borders of BCC since it reduces the time spent in surgery.

#### Quantification of Microscopic Strain on Mouse Carotid Arteries:

Sutton and colleagues (Sutton et al., 2008) used a microscopic 3D DIC system to quantify the strain field on mouse carotid arteries. By doing so local changes in bio-mechanical response of the vessel were figured out. This is because microscale alterations (strains) in the structure and composition of vessel wall results in changes in bio-mechanical response. 3D DIC utilizing a stereomicroscope was adapted to measure 3D displacements. The artery was pressurised and de-pressurised cyclically and synchronised images of them were acquired using cameras. The advantages in using a 3D DIC technique to characterise the properties of small blood vessels were described as follows:

1. Even local changes in bio-mechanical response could be quantified which helps to understand material properties of non-homogenous materials like vascular tissues;
2. This method has got a very good spatial resolution;
3. This method is highly suitable to measure strains on specimens having a curved shape (cylindrical structured blood vessels) and specimens that undergo out of plane displacements; and
4. High speed measurements at rates upto 20,000 frames are possible enabling the characterization of transient variations in biological specimens.

#### 4.2.2 On Artificial Substrates (Scaffolds)

##### Quantification of Cell Traction Forces on a Substrate:

Cell traction forces (CTF) exerted by a cell on its substrate results in deformation of the substrate. It is this deformation caused by CTF which assists in regulating many basic cellular activities like cell migration, tissue morphogenesis, wound retraction etc. Thus CTF are of prime importance to assess the cellular mechanical characteristics. Huang et al., (2008) employed a DIC technique to obtain the deformation field induced by a single cardiac myocyte on its substrate. Cells were cultured on an elastic gel substrate and they were allowed to exert mechanical forces (CTF) to deform this substrate. The elastic gel substrate was marked by randomly embedded fluorescent microbeads in order to track the deformation of the substrate. Random fluorescent patterns of beam embedded substrate captured before and after deformation induced by cell activity serves as 2 consecutive images (reference and deformed image) for processing. Image processing algorithms such as optical flow algorithm and particle tracking method were used for quantifying the displacement field. Accuracy of the obtained displacement fields can be extended to sub-pixel scale by implementation of sub-pixel registration algorithms such as newton raphson method, gradient based algorithm, correlation co-efficient curve fitting approach, etc.

#### 4.3 On other types of specimens (Metals)

##### Strain Measurement on Pure Titanium:

Toussaint and colleagues (Toussaint et al., 2008) measured the full field strain distribution of commercially pure titanium using DIC when subjected to tensile tests in order to figure out the intrinsic behaviour (stress – strain relationship) of the material. The strain fields obtained with increasing heterogeneity has been compared with the numerical results obtained from finite element analysis (simulation of the behaviour of titanium by introducing the material parameters of the elasto-plastic model into the finite element code). The satisfactory match between these results is utilised to detect the mechanical properties of titanium more accurately which allowed optimizing the design of bio-medical (titanium based) implants.

### Measurement of Mechanical Response of Welds:

Reynolds and co-workers (Reynolds et al., 1999) applied the DIC technique to measure the mechanical response of welds (heterogeneous material). The mechanical data for different micro-structural regions (fusion zone, heat affected zone and base metal zone) that makes a weld was obtained by using the DIC method. The displacements fields exhibiting the mechanical behaviour of each region were determined by correlating the images (using DIC) obtained from the surface of transversely loaded weld specimens. Unlike other tests used for testing the mechanical behaviour of welds that uses miniature specimens excised from each region in the weld, it has been reported that DIC technique uses only a single tensile test to quantify the constitutive mechanical behaviour of all regions that makes a weld.

### Deformation Measurement in a Cold Worked Material:

More recently, Kamaya and Kawakubo (2011) used DIC to measure strain at the minimum diameter position of hourglass shaped specimens subjected to tensile tests in order to obtain the post necking strain. Since post necking strain is essential to figure out the deformation of the cold worked material, hourglass shaped specimens which resemble the necking zone (of the cold worked material) were specifically used. Two cameras (3D DIC) were used to measure the strain distribution of the curved surface.

## 5 PROBLEMS ENCOUNTERED IN DIC

### 5.1 Fundamental problems in DIC

Since Image matching is an important process that helps in determining the deformations on the object's surface it becomes a great concern when two images are correlated. There follows a description of some of the major problems that occurs during image matching (after Sutton et al., 2009).

#### 5.1.1 Aperture problem

As discussed in the above section, undeformed subsets of the reference image should be compared with corresponding deformed subsets to detect the displacements between them. But practically it is difficult to find the correspondence between them when pixel level (instead of subset level) comparison is carried out. There exists a lack of unique correspondence between them, since the gray values of pixels in the reference image cannot be matched accurately with the gray values of pixels in the deformed image. This is because tracking of pixels in the reference image among the pixels in the deformed image cannot be done perfectly. In order to avoid this problem, pixels in the reference image are searched among the neighbouring pixels surrounding the pixels of interest in the deformed image. Eventhough the additional information provided by the surrounding pixels helps in this searching process, still there is an absence of unique matching. This problem could be illustrated by a single line on an image. A single point on this line is considered on the reference image which matches random points on the deformed image. This is known as aperture problem. But when the aperture is increased, the end points of the line (in the reference image) are made known. Thus the displacement vector is accurately determined since perfect mapping of points (in the deformed image) is achieved.

.....

**Figure 5-1** Aperture problem a. A point on the line can match arbitrary points on the displaced line. b. The aperture has been enlarged to include the end points of the line (Sutton et al, 2009).

### 5.1.2 Correspondence problem

Correspondence problem is nothing but figuring out the correspondence of a set of points in the first image (reference image) in the second image (deformed image) thereby identifying similar points between them. This is achieved by searching those similar points and matching them from the first image with the second image. This enables the calculation of the amount of transformation between a pair of images. This problem arises when a number of cameras are used to obtain the images of the same scene or when a single camera is used to track the relative motion of a single scene or when taking an image of an object that undergoes motion (deformation) or when there exists a time lapse when images are taken or when the camera undergoes motion. Basically there are 2 ways to find the correspondence between 2 images; correlation based and feature based. Correlation based one finds the correspondence of a specific location between the two images while feature based one finds the correspondence between the features in the reference and deformed images that is essential to quantify deformations accurately. When the material has a repeating structure (grid comprising dots or lines), a unique correspondence can be obtained provided if the aperture size is increased. When the material has a textureless structure, there is lack of correspondence since the material lacks features.



.....  
**Figure 5-2** Correspondence problem a. A repeating structure, where a unique correspondence can only be found if the edge of the grid is included in the aperture b. A textureless deforming structure, where no correspondence can be established without further assumptions (Sutton et al, 2009).

## 5.2 Practical problems in DIC

The basic concepts (theory) and the implementation of DIC technique on different types of specimen have been discussed so far. But during practical measurement of either microscale or macroscale deformations, several problems (errors) arises that has a great influence on the accuracy of strain or displacement results. Some of those problems and their solutions are discussed below:

### 5.2.1 Improvement in accuracy

Jin and co-workers (Jin et al., 2005) introduced a new technique, which they referred to as point-wise DIC, which is quite different from conventional DIC technique in several important respects. Conventional DIC method employs a subset based correlation algorithm in which subsets (a small portion of an image) of an initially undeformed image are matched with the subsets of a deformed image to determine the net displacement. Pointwise DIC, on the other hand, is capable of determining the displacement of each pixel independently, that is, displacements are determined with sub-pixel accuracy. Pointwise DIC, when implemented on real images obtained from polycarbonate dogbone specimen, indicated an inherent accuracy in measured displacements. This method has the capability of determining even discontinuous displacements more accurately, as was found when this technique was implemented on an ideal image simulating a twinning deformation. In order to determine intensity values at sub-pixel locations, bi-cubic interpolation scheme was employed.

Correlation functions were modified in order to include intensity gradients instead of intensity values which enhanced the accuracy of this technique. Thus this technique elevates accuracy of measured displacements that makes it a better technique than a conventional DIC.

### 5.2.2 Out of plane displacements

In general, DIC performed using a single camera has been widely used to measure in-plane displacements and strain. If there occurs an out of plane displacement, there arises a question of how to measure such displacements. If there is an occurrence of out of plane displacements in a system that is strictly designed to measure in-plane displacements, it causes a change in magnification of the imaging system. This eventually leads to an apparent in-plane displacement that ultimately causes an error in measurement. Tay and colleagues (Tay et al., 2005) proposed a method to calculate this apparent in-plane displacement caused due to an unknown out of plane displacement using DIC. This was achieved by employing DIC method on speckle images captured before and after the occurrence of an unknown out of plane displacement. The out of plane displacement was determined using a pinhole camera model and the calculated in-plane displacement. The method utilised a single camera to measure such 2D out-of-plane displacements. This method is suitable for measuring both structured and slightly non-structured objects.

### 5.2.3 Lens aberration

An image distortion due to optical aberration resulting in the measurement of “virtual displacements and strains” becomes a great concern when DIC is applied to micro-scale applications. When DIC is applied to macro-scale applications, image distortions caused due to lens aberration becomes negligible. But in micro-scale applications, the object is very close to lens and it is necessary that observations should be conducted under higher magnifications. Thus it is mandatory to consider the effects of lens aberration on displacement (or strain) measurement results under such conditions. Zhang et al., 2006 found a solution to this problem by adopting a simple calibration procedure in order to remove image distortions attributed to lens and prisms of light microscope. Here, a standard light microscope is considered for

which the aberration distribution is evaluated. This is done achieved by constructing a 3<sup>rd</sup> order polynomial warping function to describe the distortion errors by comparing node locations in the acquired images and the use of a simple calibration procedure that incorporates a fine pitched orthogonal cross-grating plate. Micro-tensile experiments were conducted on 3 types of materials such as aluminium, brass and a stainless sheet utilizing a microscopic imaging system. An automatic DIC algorithm has been used to determine in-plane displacements or strains by analyzing the sequential images of the specimen. Elastic modulus, strain distribution and tensile stress of these materials were evaluated which are in good agreements with the expected values. Thus this paper suggests that application of DIC to measure microscopic strains and displacements is highly feasible provided that an adequate correction is employed for image distortion.

#### 5.2.4 Computational efficiency

Acquisition of full field surface deformation using a straight forward conventional DIC algorithm is time consuming due to computational complexity. Huang and colleagues (Huang et al., 2010) introduced a new fast algorithm for which the computational efficiency is about 10-20 times higher than the conventional algorithm. In general full field surface deformation measurement involves 2 steps, location of integer pixel displacements of reference subsets and extension of the obtained results from previous step to sub-pixel level. Thus the overall time consumed to quantify the cell substrate displacement acquisition is the sum of time taken to complete integer pixel calculation and sub-pixel calculation. Sub-pixel displacement calculation is carried out by adopting sub-pixel registration algorithms like peak finding, newton raphson, spatial gradient based algorithms. Processing time of sub-pixel registration algorithms is 1% less than the time taken for integer pixel calculation. Thus accelerating the efficiency of traditional DIC relies on reducing the complexity of integer pixel correlation computation. This paper focuses in attaining this target. Adoption of the ZNCC criterion in order to accomplish integer pixel calculation is very common in a conventional DIC algorithm. This criterion has been simplified: the 2-dimensional cross-correlation term arising in the numerator of ZNCC formula was replaced by a series of basis functions and the remaining terms

are directly computed by applying sum table scheme. This dramatically reduces the computational complexity of integer pixel correlation calculation which in turn minimises the overall time required to acquire the cell-substrate displacement.

## 5.3 Errors in DIC

### 5.3.1 Errors due to speckle pattern

Pan and colleagues (Pan et al., 2008) investigated the influence of speckle pattern (information carriers of DIC) on the errors in displacement measurements of DIC method. Displacement errors in DIC associated with speckle patterns were grouped into two components: systematic errors (mean bias errors) and random errors (standard deviation errors). A theoretical model was proposed which suggested that only random errors (quantified by standard deviation displacement measurement error) were introduced by the speckle patterns used in DIC (implemented using Newton Raphson algorithm) and systematic errors were not a part of its influence. In order to validate this phenomenon derived by this model five different speckle patterns each with different intensity distribution were analysed and the results matches the suggestion given by the theoretical model i.e systematic errors were influenced only by intensity interpolation errors(errors due to sub-pixel position of the displaced subset) but not due to speckle patterns. It has also been observed that these random errors can be minimised by choosing a large subset.

### 5.3.2 Errors due to Intensity Interpolation

As pointed out by Schreier et al. (2000) interpolation phase errors may introduce errors in the strain measurements. Images of two speckle patterns, one exhibiting a continuous (but uniform) gray level distribution and another with bi-modal gray level (intensity) distribution were applied with different types of interpolation schemes like cubic polynomial, cubic spline and quintic spline and were examined. A high amount of errors (interpolation errors) were observed in the speckle patterns with a bi-modal gray level distribution and very less amount of were observed in the speckle patterns with a uniform intensity distribution. The minimum error was of the order of 4% was indicated when a cubic polynomial interpolation was applied on the

speckle pattern with continuous intensity distribution whereas the minimum error was of the order of 15% when a quintic spline interpolation applied on the speckle pattern with bi-modal gray level distribution. These errors were attributed to the phase errors introduced by interpolation schemes. It was also found that linear interpolation schemes introduced a higher rate of strain measurement errors (due to increase in phase errors) than the other higher order interpolation schemes. Thus, in order to minimise these phase errors, higher orders interpolation methods (cubic interpolation scheme) were preferred. Moreover, low pass filtering the speckle images before correlation process has been suggested as a good solution to reduce these phase errors.

### 5.3.3 Errors due to experimental setup and DIC algorithms

Haddadi and Belhabib (2008) investigated different sources of errors that could possibly occur during DIC application by subjecting an undeformed sample to a rigid body motion. Most of the errors were due to problems linked with quality of experimental devices, working environment and correlation principle. This includes errors caused due to lighting, CCD sensor, optical lens distortion, presence of out of displacement, arrangement of devices required for DIC in workspace , quality of speckle pattern, correlation algorithm, selective parameters related with correlation principle (grid pitch, subset size, type of correlation criterion used etc.). Many suggestions were emphasized to minimise these errors in order to reduce their effects on strain results.

After analysis it has been found that, the major source of error occurs due to the presence of out of plane displacement. This could be reduced by using stereo correlation or using a telecentric lens. Errors due to light variation changes the gray levels of the acquired images which decrease the correlation accuracy. This could be minimised when a uniform and sufficient light that covers the whole zone of interest of the sample surface was provided. Errors due to speckle pattern can occur if its quality is not adequate, which could be reduced by using an optimised pattern. Choice of subset size causes errors in many situations. If the subset size is small it leads to wrong correlation. If the subset size is large, quality of correlation is high but

quality of measurement is low. This is due to the increase in the computation time. Thus the subset size must be chosen in a way that both the accuracy and computation time are compromised. Errors may occur due to a wrong choice of grid pitch which could be minimised by using an optimised grid pitch. When these errors that occur due to the experimental arrangements are corrected, the strain results obtained using DIC would be of better quality and high accuracy.

## 6 CONCLUSION

In this review, the effectiveness and suitability of DIC for microscale strain mapping in scaffolds and its importance for predicting the characteristics of scaffolds has been discussed. A brief overview of the different processes and equipments used for DIC implementation, including the problems encountered and their possible solutions has been described. Future work in use of DIC for micro strain measurements should ideally take into consideration the points emphasised below for precise and reliable measurements.

## 7 FUTURE WORK

### 7.1 Optimised Specimen Surface Preparation

Since in microscopic strain measurements, the sample size is very small and we use optical methods to measure strain, the specimen surfaces should not have any form of artefacts. Even very small amounts of dirt or stains can cause major offset in the accuracy of measurement. Hence, the specimen is cleaned and processed well. The processing method entirely depends on the type of specimen used, which can be bone, visceral tissues, skin or brain tissues etc. The speckle pattern using paint is applied to create a unique random pattern, which aids in Image correlation with a narrow margin of errors.

### 7.2 Improvements in image acquisition

While using 2D scaffolds, cell traction forces can be measured using 2D microscopes, with relatively high accuracy. Whereas, when 3D scaffolds are used, there is a 3 dimensional volumetric mesh with a complex architecture. Hence, there are a number of out of plane displacements. If 2D microscopes are used, the out of plane displacements would lead to a drastic offset in displacement measurements. Hence we require 3D image visualization techniques like confocal microscopy or microCT to analyse the 3D displacements. Improvement in image acquisition is purely hardware dependant. Hence the properties of the acquired images will rely on the type of hardware used to acquire the image.

### 7.3 Optimisation of Image Registration

As discussed previously, either of these methods have their own advantages. For instance Feature based method has more specificity and Intensity based method has more sensitivity. When scaffolds are used for image registration, we can see that they have abundance of fibres in different patterns and under a microscope and these fibres are seen to have high contrast. So, if the intensity based method is used, the specificity maybe lost. Also, since the fibres are in varying patterns, if we use feature



based matching for registering the scaffolds, the sensitivity may be lost. Hence, when we need the highest amount of accuracy, we need to combine these methods to get optimum results.

## 7.4 Image Processing

2D and 3D images, though acquired through different image acquisition equipments, similar DIC techniques and similar principles for data analysis, are employed in most cases. 2D DIC methods use a single plane measurement system for displacement measurements. Whereas, the 3D DIC methods utilise a volumetric approach and require extensive amount of processing power and speed. And moreover, future scaffolds were expected to have a 3D architecture which assists in creating a better physiological environment. These 3D scaffolds create a lot of out of plane displacements which cannot be measured precisely using 2D DIC. Thus 3D DIC becomes mandatory for future work for measuring 3D scaffold displacements accurately.

## 7.5 Algorithms and Schemes

Of all the above correlation criteria discussed in Table 1 and 2, since zero normalised CC and SSD criteria are insensitive to both offset and scale changes, they should be used to establish better correspondence between the reference and the target subset gray scale intensities. Concerned with interpolation schemes, bi-linear and bi-cubic interpolation schemes can offer better and more accurate sub-pixel displacement measurements, since they aim to track sub-pixel points that is a weighted average of  $2 \times 2$  and  $4 \times 4$  surrounding integer pixels. Regarding sub-pixel displacement measurement algorithms, Newton Raphson scheme is an algorithm which utilises iteration scheme that calculates successive orders of grayscale intensities using previously obtained grayscale intensity. Combined approach that adopts Newton Raphson algorithm and bi-cubic interpolation scheme goes well, since the realization of the NR scheme is possible only with smooth sub-pixel grayscale intensity values which can be easily provided by our bi-cubic interpolation scheme.

## 7.6 Improvement in Strain and Displacement Measurement Accuracy

DIC has been proven to be very accurate in many experiments where real-time displacement measurements done using conventional methods have been compared with microstrain measurements using DIC. It is quite understandable that multiple algorithms can be used and several thousandth of a pixel can be interpolated, but all this comes at the cost of the computational efficiency and processing time. So, ideally, the range of accuracy expected in the experiments and the amount of acceptable errors must be well known before the image processing methods are chosen. Based on the above criteria, the sensitivity and specificity of the experiment is balanced and then the displacement and strain measurements are found. The best method of improving accuracy is by using a very high resolution camera sensor, thereby reducing the requirements of high end interpolation techniques and better accuracy.

# REFERENCES

## JOURNALS AND ARTICLES

Ananthakrishnan R, Ehrlicher A. The Forces behind Cell Movement. *International Journal of Biological Sciences* 2007; 3:303-317.

Bing P, Hui-min X, Bo-qin X, Fu-long D. Performance of sub-pixel registration algorithms in digital image correlation. *Measurement Science and Technology* 2006; 17:1615-1621.

Brown L.G. A Survey of Image Registration Techniques. *ACM Computing Surveys* 1992; 24:325-376.

Chan B.P., Leong K.W. Scaffolding in tissue engineering: general approaches and tissue-specific considerations. *Eur Spine J* 2008; 17:467-479.

Chen G, Ushida T, Tateishi T. Scaffold Design for Tissue Engineering. *Macromolecular Bioscience* 2002; 2:67-77.

Curtis A, Sokolikova-Csaderova L, Aitchison G. Measuring Cell Forces by a Photoelastic Method. *Biophysical Journal* 2007; 92:2255-2261.

Da Fonseca J.Q., Mummery P.M., Withers P.J. Full-field strain mapping by optical correlation of micrographs acquired during deformation. *Journal of Microscopy* 2004; 218:9-21.

Dahl K.N., Ribeiro A.J.S., Lammerding J. Nuclear Shape, Mechanics, and Mechanotransduction. *Circulation Research* 2008; 102:1307-1318.

Dhandayuthapani B, Yoshida Y, Maekawa T, Kumar D.S. Polymeric Scaffolds in Tissue Engineering Application: A Review. *International Journal of Polymer Science* 2011; 2011: Article ID 290602.

Evans S.L., Holt C.A. Measuring the mechanical properties of human skin in vivo using digital image correlation and finite element modelling. *The Journal of Strain Analysis for Engineering Design* 2009; 44:337-345.

Gabbiani G, Ryan GB, Majno G (1971) Presence of modified fibroblasts in granulation tissue and their possible role in wound contraction. *Experientia* 27: 549–55

Ghosh K, Ingber D.E. Micromechanical control of cell and tissue development: Implications for tissue engineering. *Advanced Drug Delivery Reviews* 2007; 59:1306-1318.

Haddadi H, Belhabib S. Use of rigid-body motion for the investigation and estimation of the measurement errors related to digital image correlation technique. *Optics and Lasers in Engineering* 2008; 46:185-196.

Hahn C, Schwartz M.A. Mechanotransduction in vascular physiology and atherogenesis. *Nat Rev Mol Cell Biol* 2009; 10:53-62.

Hamilton A.R., Sottos N.R., White S.R. Local Strain Concentrations in a Microvascular Network. *Experimental Mechanics* 2009; 50:255-263.

Harris A.K., Wild P, Stopak D. Silicone Rubber Substrata: A New Wrinkle in the Study of Cell Locomotion. *Science* 1980;208:177-179.

Heinz S.R., Wiggins J.S. Uniaxial compression analysis of glassy polymer networks using digital image correlation. *Polymer Testing* 2010; 29:925-932.

Holy CE, Cheng C, Davies JE, Shoicet MS. Optimization of PGLA scaffolds for use in tissue engineering. PMID11085380. *Biomaterials* 2001;22(1):25-31.

Huang C, Ogawa R. Mechanotransduction in bone repair and regeneration. *The FASEB Journal* 2010; 24:3625-3632.

Huang J, Pan X, Peng X, Zhu T, Qin L, Xiong C, Fang J. High-efficiency cell–substrate displacement acquisition via digital image correlation method using basis functions. *Optics and Lasers in Engineering* 2010; 48:1058-1066.

Ingber D.E. Mechanobiology and diseases of mechanotransduction. *Annals of medicine* 2003; 35:1-14.

Ingber D.E. Cellular mechanotransduction: putting all the pieces together again. *The FASEB Journal* 2006; 20:811-827.

Kamaya M, Kawakubo M. A procedure for determining the true stress–strain curve over a large range of strains using digital image correlation and finite element analysis. *Mechanics of Materials* 2011; 43:243-253.

Kazemnejad S. Hepatic Tissue Engineering Using Scaffolds: State of the Art. *Avicenna Journal of Medical Biotechnology* 2009; 1:135-145.

Kerl J, Parittotokkaporn T, Frasson L, Oldfield M, y Baena F.R., Beyrau F. Tissue deformation analysis using a laser based digital image correlation technique. *Journal of the Mechanical Behavior of Biomedical Materials* 2012; 6:159-165.

Krehbiel J.D., Lambros J, Viator J.A., Sottos N.R. Digital Image Correlation for Improved Detection of Basal Cell Carcinoma. *Experimental Mechanics* 2010; 50:813–824.

Lauret C, Hrapko M, van Dommelen J.A. , Peters G.W., Wismans J.S. Optical characterization of acceleration-induced strain fields in inhomogeneous brain slices. *Medical Engineering and Physics* 2009; 31:392-399.

Lecomptea D, Smitsb A, Bossuytb S, Solb H, Vantommea J, Van Hemelrijckb D, Habraken A.M. Quality assessment of speckle patterns for digital image correlation. *Optics and Lasers in Engineering* 2006; 44:1132-1145.

Libertiaux V, Pascon F, Cescotto S. Experimental verification of brain tissue incompressibility using digital image correlation. *Journal of the Mechanical Behavior of Biomedical Materials* 2011; 4:1177-1185.

Mammoto T, Ingber D.E. Mechanical control of tissue and organ development. *Development* 2010; 137:1407-1420.

Maruthamuthu V, Sabassb B, S. Schwarzb U.S., Gardela M.L. Cell-ECM traction force modulates endogenous tension at cell–cell contacts. *Proceedings of the National Academy of Sciences of the United States of America* 2011; 108:4708-4713.

McCain M.L., Parker K.K. Mechanotransduction: the role of mechanical stress, myocyte shape, and cytoskeletal architecture on cardiac function. *Pflugers Arch - Eur J Physiol* 2011; 462:89-104.

Nemeno-Guanzon J.G., Lee S, Berg J.R., Jo Y.H., Yeo J.E., Nam B.M., Koh Y-G, Lee J.I. Trends in Tissue Engineering for Blood Vessels. *Journal of Biomedicine and Biotechnology* 2012; 2012: Article ID 956345.

O'Brien F.J. Biomaterials and scaffolds for tissue engineering. *Materials Today* 2011; 14:88-95.

Pan B. Recent Progress in Digital Image Correlation. *Experimental Mechanics* 2011; 51:1223-1235.

Pan B, Qian K, Xie H, Asundi A. Two-dimensional digital image correlation for in-plane displacement and strain measurement: a review. *Measurement Science and Technology* 2009; 20:1-17.

Prajapati A, Naik S, Mehta S. Evaluation of Different Image Interpolation Algorithms. *International Journal of Computer Applications* 2012; 58:6-12.

Sahoo S, Cho-Hong J.G., Siew-Lok T. Development of hybrid polymer scaffolds for potential applications in ligament and tendon tissue engineering. *Biomedical Materials* 2007; 2:169-173.

Saleem Q, Wildman R.D., Huntley J.M., Whitworth M.B. Improved understanding of biscuit checking using speckle interferometry and finite-element modelling techniques. *Proceedings of the Royal Society A* 2005; 461:2135-2154.

Sutton M.A., Ke X, Lessner S.M., Goldbach M, Yost M, Zhao F, Schreier H.W. Strain field measurements on mouse carotid arteries using microscopic three-dimensional digital image correlation. *Journal of Biomedical Materials Research Part A* 2008; 84:178-190.

Sztefek P, Vanleene M, Olsson R, Collinson R, Pitsillides A.A., Shefelbine S. Using digital image correlation to determine bone surface strains during loading and after adaptation of the mouse tibia. *Journal of Biomechanics* 2010; 43:599-605.

Tanasic I, Milic-Lemic A, Tihacek-Sojic L, Stancic I, Mitrovic N. Analysis of the compressive strain below the removable and fixed prosthesis in the posterior mandible using a digital image correlation method. *Biomech Model Mechano Biol* 2012; 11:751-758.

Tang Z, Liang J, Xiao Z, Guo C. Large deformation measurement scheme for 3D digital image correlation method. *Optics and lasers in engineering* 2012; 50:122-130.

Tay C.J., Quan C, Huang Y.H., Fu Y. Digital image correlation for whole field out-of-plane displacement measurement using a single camera. *Optics Communications* 2005; 251:23-36.

Tong W. Plastic Surface Strain Mapping of Bent Sheets by Image Correlation. *Experimental Mechanics* 2004; 44:502-511.

Toussaint F, Tabourot L, Vacher P. Experimental study with a Digital Image Correlation (DIC) method and numerical simulation of anisotropic elastic-plastic

commercially pure titanium. Archives of Civil and Mechanical Engineering 2008; 8:131-143.

Vogel V, Sheetz M. Local force and geometry sensing regulate cell functions. Nature Reviews Molecular Cell Biology 2006; 7:265-275.

Wang C.C., Deng J.M., Ateshian G.A., Hung C.T. An Automated Approach for Direct Measurement of Two-Dimensional Strain Distributions within Articular Cartilage under Unconfined Compression. Journal of Biomechanical Engineering 2002; 124:557-567.

Wang J.H-C., Li B. The principles and biological applications of cell traction force microscopy. Microscopy: Science, Technology, Applications and Education 2010; 1:449-458.

Yamaguchi H, Kikugawa H, Asaka T, Kasuya H, Kuninori M. Measurement of Cortical Bone Strain Distribution by Image Correlation Techniques and from Fracture Toughness. Materials Transactions 2011; 52:1026- 1032.

Yoshihiro Y Abiko and Denis D Semlimovic The mechanism of protracted wound healing in on oral mucosa in diabetes. Medical Sciences 2010; 10(3):186-191.

Zhang D, Arola D.D. Applications of digital image correlation to biological tissues. Journal of Biomedical Optics 2004; 9:691-699.

Zitova B, Flusser J. Image registration methods: a survey. Image and Vision Computing 2003; 21:977-1000.

## BOOKS

Sutton M.A., Orteu J.J., Schreier H.W. Image Correlation for Shape, Motion and Deformation Measurements 2009. ISBN 978-0-387-78746-6.

Sutton M.A. Prof. Digital Image Correlation for Shape and Deformation Measurements. Sharpe W.N., Jr. Prof (Eds.), The Springer Handbook of Experimental Solid Mechanics 2008: pp565-600. Springer US: New York. ISBN 978-0-387-26883-5.

## WEBSITES

- [1]. Biomaterials: Descriptions of several materials used in the field [image online]. Available at: [biomed.brown.edu](http://biomed.brown.edu) [Accessed 7 November 2012].
- [2]. Schematic of a migrating cell and the tractions it generates on the substrate [image online]. Available at: [cellmigration.org](http://cellmigration.org) [Accessed 26 December 2012].
- [3]. "Combi" approaches for screening a wide range of 3D scaffolds have been developed to comprise a "scaffoldomics" approach [image online]. Available at: [nist.gov](http://nist.gov) [Accessed 31 December 2012].
- [4]. Bone cells attach to scaffolds by extending cell processes to the surface [image online]. Available at: [itg.beckman.illinois.edu](http://itg.beckman.illinois.edu) [Accessed 24 December 2012].
- [5]. Antimicrobial scaffolds for tissue engineering [image online]. Available at: [materialsviews.com](http://materialsviews.com) [Accessed 27 November 2012].
- [6.] 3D-Fect™- 3D Transfection: a new outlook for your cells [image online]. Available at: [ozbiosciences.com](http://ozbiosciences.com) [Accessed 18 December 2012].
- [7]. Schematic diagram of the strain measurement system using a laser extensometer and a hydraulic clamping specimen holder [image online]. Available at: [jolisfukyu.tokai-sc.jaea.go.jp](http://jolisfukyu.tokai-sc.jaea.go.jp) [Accessed on 20 December 2012].
- [8]. Laser extensometer –laser Xtens [image online]. Available at: [directindustry.com](http://directindustry.com) [Accessed 29 December 2012].
- [9]. A typical speckle pattern [image online]. Available at: [cranfield.ac.uk](http://cranfield.ac.uk) [Accessed 19 November 2012].
- [10]. Aortic specimen, showing speckle for DIC [image online]. Available at: [ul.ie](http://ul.ie) [Accessed 17 November 2012].
- [11]. 5 Megapixel GigE and USB industrial cameras with CCD or CMOS sensors [image online]. Available at: [news.directindustry.com](http://news.directindustry.com) [Accessed 31 December 2012].
- [12]. Olympus SZ60 stereo microscope from Olympus [image online]. Available at: [olympusmicro.com](http://olympusmicro.com) [Accessed 22 November 2012].
- [13]. Basic configuration of the first micro-CT scanner- Evolution of PIRL Micro-CT Scanning [image online]. Available at: [mayoresearch.mayo.edu](http://mayoresearch.mayo.edu) [Accessed 20 October 2012].



- [14]. The Skyscan-1172 micro-CT Scanner from Bruker[image online]. Available at: [skyscan.be](http://skyscan.be) [Accessed 21 October 2012].
- [15]. Scanning Electron Microscope-working [image online]. Available at: [purdue.edu](http://purdue.edu) [Accessed 23 November 2012].
- [16]. Electron microscope [image online] from Hitachi model S-3500N LVSEM . Available at: [labx.com](http://labx.com) [Accessed 12 October 2012].
- [17]. FV1200 LASER Scanning Confocal Microscope from Olympus America [image online]. Available at: [olympusamerica.com](http://olympusamerica.com) [Accessed 16 November 2012].
- [18]. Laser Scanning Confocal Microscopy [image online]. Available at: [med.unc.edu](http://med.unc.edu) [Accessed 10 December 2012].
- [19]. Digital image interpolation (Bi-cubic and bi-linear interpolation) [image online]. Available at: [cambridgeincolour.com](http://cambridgeincolour.com) [Accessed 10 December 2012].
- [20]. Set-up for 3D digital image correlation [image online]. Available at: [lib.znate.ru](http://lib.znate.ru) [Accessed 24 October 2012].
- [21]. Strain evaluation [image online]. Available at: [lavision.de](http://lavision.de) [Accessed 10 October 2012].

#### CONFERENCE PAPERS

- Bland M.E., Cortes M, Solt K.J., Siadat M, Yang L. Stereo Digital Image Correlation for the Characterization of Fresh Biomaterials. Photonic Therapeutics and Diagnostics VI (754847) 2010. DOI:10.1117/12.839881.
- Cofaru C, Philips W and Paepegemb W.V. A three-frame digital image correlation (DIC) method for the measurement of small displacements and strains. Measurement science and technology 2012. DOI:10.1088/0957-0233/23/10/105406.
- Hercher M, Wyntjes G, DeWeerd H. Non-contact laser extensometer. Industrial laser interferometry 1987. DOI:10.1117/12.939780.
- Htwe A.N. Image Interpolation framework using non-adaptive approach and NL means. International Journal of Network and Mobile Technologies 2010, volume 1. ISSN 1832-6758 electronic version.

Huang J, Wu J, Qin L, Zhua T, Xiong C, Zhang Y, Fang J. Mechanical Behaviour Study of Single Cell Contraction by Digital Image Correlation Technique. International Conference on Experimental Mechanics 2008. DOI:10.1117/12.839324.

Jin H, Bruck H.A. Theoretical development for pointwise digital image correlation. Optical Engineering 2005. DOI:10.1117/1.1928908.

Lecompte D, Bossuyt S, Cooreman S, Sol H, Vantomme J. Study and generation of optimal speckle patterns for DIC. Proceedings from the 2007 SEM conference. Available from: <http://sem-proceedings.com/07s/sem.org-2007-SEM-Ann-Conf-s73p01-Study-Generation-Optimal-Speckle-Patterns-DIC.pdf>.

Mates S.P., Rhorer R. High Strain Rate Tissue Simulant Measurements Using Digital Image Correlation. Proceedings of the SEM Annual Conference 2009. Available from : <http://sem-proceedings.com/09s/sem.org-SEM-2009-Ann-Conf-s020p01-High-Strain-Rate-Tissue-Simulant-Measurements-Using-Digital-Image.pdf>

Pan B, Qian K, Xie H, Asundi A. On errors of digital image correlation due to speckle patterns. International Conference on Experimental Mechanics 2008. DOI:10.1117/12.839326.

Reynolds A.P., Duvall F. Digital Image Correlation for Determination of Weld and Base Metal Constitutive Behavior. Welding Research Supplement, 355s - 360s, 1999.

Schreier H.W., Braasch J.R., Sutton M.A. Systematic errors in digital image correlation caused by intensity interpolation. Optical Engineering 2000. DOI:10.1117/1.1314593.

Subia B, Kundu J, Kundu S.C. Biomaterial Scaffold Fabrication Techniques for Potential Tissue Engineering Applications. Tissue Engineering 2010. Daniel Eberli (Ed.), ISBN: 978-953-307-079-7, DOI: 10.5772/8581.

Tang Z-Z, Liang J, Xiao Z-Z, Guo C, Hu H. Three-dimensional digital image correlation system for deformation measurement in experimental mechanics. Optical engineering 2010. doi:10.1117/1.3491204.

Xiong L, Liu X, Liu G, Liu J, Yang X, Tan Q. Evaluation of Sub-pixel Displacement Measurement Algorithms in Digital Image Correlation. International Conference on Mechatronic Science, Electric Engineering and Computer 2011, pp 1066-1069. Print ISBN: 978-1-61284-719-1.

Zhang D, Luo M, Arola D.D. Displacement/strain measurements using an optical microscope and digital image correlation. *Optical Engineering* 2006. DOI:10.1117/1.2182108.



